

Reconsidering the *One Leptoquark* solution: flavor anomalies and neutrino mass

Yi Cai,^a John Gargalionis,^a Michael A. Schmidt^b and Raymond R. Volkas^a

^a*ARC Centre of Excellence for Particle Physics at the Terascale,
School of Physics, The University of Melbourne, Victoria 3010, Australia*

^b*ARC Centre of Excellence for Particle Physics at the Terascale,
School of Physics, The University of Sydney, NSW 2006, Australia*

E-mail: yi.cai@unimelb.edu.au, garj@student.unimelb.edu.au,
michael.schmidt@sydney.edu.au, raymondv@unimelb.edu.au

ABSTRACT: We reconsider a model introducing a scalar leptoquark $\phi \sim (\mathbf{3}, \mathbf{1}, -1/3)$ to explain recent deviations from the standard model in semileptonic B decays. The leptoquark can accommodate the persistent tension in the decays $\bar{B} \rightarrow D^{(*)}\tau\bar{\nu}$ as long as its mass is lower than approximately 10 TeV, and we show that a sizeable Yukawa coupling to the right-chiral tau lepton is necessary for an acceptable explanation. A characteristic prediction of this scenario is a value of R_{D^*} slightly smaller than the current world average. Agreement with the measured $\bar{B} \rightarrow D^{(*)}\tau\bar{\nu}$ rates is mildly compromised for parameter choices addressing the tensions in $b \rightarrow s\mu\mu$, where the model can significantly reduce the discrepancies in angular observables, branching ratios and the lepton-flavor-universality observables R_K and R_{K^*} . The leptoquark can also reconcile the predicted and measured value of the anomalous magnetic moment of the muon and appears naturally in models of radiative neutrino mass derived from lepton-number violating effective operators. As a representative example, we incorporate the particle into an existing two-loop neutrino mass scenario derived from a dimension-nine operator. In this specific model, the structure of the neutrino mass matrix provides enough freedom to explain the small masses of the neutrinos in the region of parameter space dictated by agreement with the anomalies in $\bar{B} \rightarrow D^{(*)}\tau\bar{\nu}$, but not the $b \rightarrow s$ transition. This is achieved without excessive fine-tuning in the parameters important for neutrino mass.

Contents

1	Introduction	1
2	The scalar leptoquark model	4
3	Phenomenological analysis	5
3.1	Signals	5
3.1.1	Charged current processes	6
3.1.2	Neutral current processes	8
3.1.3	Anomalous magnetic moment of the muon	10
3.2	Constraints	11
3.2.1	Semileptonic charged current processes	12
3.2.2	Lepton flavor violating processes	15
3.2.3	Rare meson decays	17
3.2.4	Meson mixing	21
3.2.5	Precision electroweak measurements	22
4	Results and discussion	22
4.1	Flavor anomalies	23
4.2	A representative neutrino mass realization	32
5	Conclusions	35

1 Introduction

Recently, measurements in the decays of B mesons have established a number of significant and unresolved deviations from the predictions of the standard model (SM). Many of these involve rare flavor changing neutral current (FCNC) $b \rightarrow s$ transitions. An important example is the LHC***b*** collaboration’s measured suppression in the ratios

$$R_{K^{(*)}} = \frac{\Gamma(\bar{B} \rightarrow \bar{K}^{(*)} \mu^+ \mu^-)}{\Gamma(\bar{B} \rightarrow \bar{K}^{(*)} e^+ e^-)}, \quad (1.1)$$

hinting towards a violation of lepton flavor universality (LFU). Although the prediction of each individual decay rate is plagued by hadronic uncertainties, these cancel out in the ratios R_K and R_{K^*} in the regime where new-physics effects are small [1–3]. In the SM the prediction of the observables outside of the low- q^2 region is determined by physics which is wholly independent of the flavor of the lepton pair in the final state, making R_K and R_{K^*} finely sensitive to violations of LFU. LHC***b*** finds [4]

$$R_K = 0.745^{+0.090}_{-0.074} \pm 0.036, \quad (1.2)$$

Experiment	R_D	R_{D^*}
BaBar [24]	$0.440 \pm 0.058 \pm 0.042$	$0.332 \pm 0.024 \pm 0.018$
Belle [26–28]	$0.375 \pm 0.064 \pm 0.026$	$0.293 \pm 0.038 \pm 0.015$
	—	$0.302 \pm 0.030 \pm 0.011$
	—	$0.270 \pm 0.035^{+0.028}_{-0.025}$
LHCb [29]	—	$0.336 \pm 0.027 \pm 0.030$
HFAG average ¹ [36]	$0.397 \pm 0.040 \pm 0.028$	$0.316 \pm 0.016 \pm 0.010$
Our average	—	0.311 ± 0.016
SM prediction	0.299 ± 0.011 [37]	0.252 ± 0.003 [38]

Table 1: A summary of results associated with $b \rightarrow c\tau\nu$. Our average includes the most recent Belle measurements of R_{D^*} , it is calculated by taking an error-weighted mean after summing statistical and systematic uncertainties in quadrature.

for dilepton invariant mass squared range $1 \text{ GeV}^2 < q^2 < 6 \text{ GeV}^2$, while the SM demands $R_K^{\text{SM}} = 1.0003 \pm 0.0001$ [5]. More recently, LHCb have also measured R_{K^*} [6]:

$$R_{K^*} = \begin{cases} 0.660^{+0.110}_{-0.070} \pm 0.024 & \text{for } 0.045 \text{ GeV}^2 < q^2 < 1.1 \text{ GeV}^2 \\ 0.685^{+0.113}_{-0.069} \pm 0.047 & \text{for } 1.1 \text{ GeV}^2 < q^2 < 6 \text{ GeV}^2 \end{cases}, \quad (1.3)$$

a deviation from the SM prediction [7] at the 10% level and a clear signpost to new physics. A number of analyses have argued that each of these $\sim 2.5\sigma$ discrepancies can be eliminated through a four-fermion effective operator $(\bar{s}\gamma_\mu P_L b)(\bar{\mu}\gamma^\mu P_L \mu)$, leading to new contributions to the muonic decay mode of the B meson [2, 8–19]. Such an effective operator can also ameliorate other tensions in the measurements of angular observables and branching ratios involving the $b \rightarrow s$ transition, although these are subject to sizeable hadronic uncertainties [20–23]. Currently, global fits suggest new physics in $(\bar{s}\gamma_\mu P_L b)(\bar{\mu}\gamma^\mu P_L \mu)$ is preferred at between 4.2 and 6.2σ [2, 16–19] over the SM, and many new-physics models attempting to explain this deviation exist.

Another intriguing anomaly is the long-standing deviation in the ratios

$$R_{D^{(*)}}^{\tau/\ell} = \frac{\Gamma(\bar{B} \rightarrow D^{(*)}\tau\bar{\nu})}{\Gamma(\bar{B} \rightarrow D^{(*)}\ell\bar{\nu})}, \quad (1.4)$$

where $\ell \in \{e, \mu\}$, reported by the BaBar [24, 25], Belle [26–28] and LHCb [29] collaborations. These measurements show a remarkable degree of self-consistency and together amount to a deviation larger than 4σ from the SM expectation [30–35]. Measurements of the dilepton invariant mass distribution disfavor many popular new physics scenarios (e.g. type-II two Higgs doublet models [24]) as candidate explanations. We present a summary of the recent experimental results and SM predictions associated with $b \rightarrow c\tau\nu$ in Table 1.

¹The HFAG average does not include the most recent Belle measurement [28].

A common origin for $R_{D^{(*)}}$ and the anomalous $b \rightarrow s$ data is suggested naturally if the former is explained by the effects of the operator $(\bar{c}\gamma_\mu P_L b)(\bar{\tau}\gamma^\mu P_L \nu)$, related in its general structure by $SU(2)_L$ invariance to the aforementioned four-fermion effective operator accounting for the $b \rightarrow s$ anomalies. A number of models exploring this idea have been suggested in the literature [39–53] (along with many others addressing one or the other anomaly, *e.g.* [11, 15, 30, 32, 54–67]) and among these minimal explanations the Bauer–Neubert (BN) model [40] is one of notable simplicity and explanatory power: a TeV-scale scalar leptoquark protagonist mediating $\bar{B} \rightarrow D^{(*)}\tau\bar{\nu}$ at tree-level and the $b \rightarrow s$ decays through one-loop box diagrams. The leptoquark transforms under the SM gauge group like a right-handed down-type quark and its pattern of couplings to SM fermions can also reconcile the measured and predicted values of the anomalous magnetic moment of the muon, another enduring tension.

Taken together, these measurements paint a picture of new physics interacting more strongly with the second and third generations of SM fermions, introducing lepton flavor non-universality and FCNC interactions at energies not significantly higher than the electroweak scale. Interestingly, many of these phenomenological motifs arise naturally in radiative models of neutrino mass, hinting towards the attractive possibility of a common explanation for both phenomena.

The disparity in scale between the masses of the charged fermions and the sub-eV neutrinos is a well-established shortcoming of the SM. A distinguishing feature is that the neutrinos may be Majorana fermions whose mass term can be generated from suitable lepton number violating effective operators when the high-scale physics is integrated out. Effective operators that violate lepton number by two units ($\Delta L = 2$) have been categorized and studied in the literature [68, 69], and a diverse landscape of models emerges by considering different completions of these in the ultraviolet (UV). The process of opening up the operators and developing renormalizable models of neutrino mass has been formalized into a minimal model building prescription [70] from which the canonical seesaw models and popular radiative scenarios emerge naturally. Previous work has also considered radiative neutrino mass models whose particle content addresses R_K [53, 62, 71–73], $R_{D^{(*)}}$ [47, 53] and $(g - 2)_\mu$ [53, 71–74]. In Refs. [47, 62] the flavor anomalies are explained through two light scalar or vector leptoquarks whose couplings to the SM Higgs doublet and fermions prohibit a consistent assignment of lepton number to the leptoquarks such that the symmetry is respected. Thus $U(1)_L$ is explicitly broken by two units and the neutrinos gain mass at the one-loop level [75], apart from the imposition of any additional symmetries². A general feature of such models is that large amounts of fine-tuning are required to suppress the neutrino mass to the required scale with at least one set of leptoquark–fermion couplings sizeable enough to explain the anomalies.

Our aim in this work is twofold: (i) to study the scalar leptoquark model in the context of some previously unconsidered constraints and comment more definitely on its viability as an explanation of both $R_{D^{(*)}}$ and $R_{K^{(*)}}$; and (ii) to build on previous work by considering a

²Mass generation in Ref. [74] occurs at the two-loop level because the Yukawa couplings of one of the leptoquarks to the left-chiral fermions is turned off.

two-loop neutrino mass model (first presented in Ref. [76]) whose particle content includes the TeV-scale scalar leptoquark present in the BN scenario. In doing so we hope to establish the explanatory power of this simple extension of the SM, emphasizing the simplicity with which it can be embedded into a radiative model of Majorana neutrino mass. We find that the two-loop scheme heavily alleviates the fine-tuning present in the one-loop models, and we expect this result to be general for all two-loop topologies.

The remainder of this work is structured as follows. Section 2 outlines the scalar leptoquark model in which the phenomenological analysis of Section 3 takes place. Within this analysis, we present the regions of parameter space interesting for the flavor anomalies in Section 3.1, relevant constraints for the model in Section 3.2 and a general discussion of our results in Section 4. Finally, in Section 4.2 we incorporate the scalar leptoquark into a representative two-loop neutrino mass model.

2 The scalar leptoquark model

The leptoquark ϕ that features in the BN model transforms under the SM gauge group as $\phi \sim (\mathbf{3}, \mathbf{1}, -1/3)$, corresponding to the leptoquark S_1 in the nomenclature of Ref. [77]. These transformation properties lead to generalized Yukawa couplings of the leptoquark to SM quarks and leptons as well as baryon number violating diquark couplings which we choose to turn off to avoid destabilizing the proton³. The part of the Lagrangian relevant to ϕ is⁴

$$\mathcal{L}_\phi = (D_\mu \phi)^\dagger (D^\mu \phi) + m_\phi^2 |\phi|^2 - \kappa |H|^2 |\phi|^2 + \hat{x}_{ij} \hat{L}_L^i \hat{Q}_L^j \phi^\dagger + \hat{y}_{ij} \hat{e}_R^i \hat{u}_R^j \phi + \text{h.c.}, \quad (2.1)$$

where H is the SM Higgs doublet, $i, j \in \{1, 2, 3\}$ are generational indices, interaction eigenstate fields are hatted and $\chi\psi = \overline{\chi^c}\psi$ for spinor fields, while $\text{SU}(2)_L$ indices have been suppressed. We move from the interaction to the charged-fermion mass basis through the unitary transformations

$$\begin{aligned} \hat{u}_L^i &= (L_u)^{ij} u_L^j, & \hat{d}_L^i &= (L_d)^{ij} d_L^j, & \hat{u}_R^i &= (R_u)^{ij} u_R^j, \\ \hat{e}_L^i &= (L_e)^{ij} e_L^j, & \hat{\nu}_L^i &= (L_e)^{ij} \tilde{\nu}_L^j, & \hat{e}_R^i &= (R_e)^{ij} e_R^j, \end{aligned} \quad (2.2)$$

where $\mathbf{V} = \mathbf{L}_u^\dagger \mathbf{L}_d$ is the Cabibbo–Kobayashi–Maskawa (CKM) matrix and the Pontecorvo–Maki–Nakagawa–Sakata (PMNS) matrix \mathbf{U} rotates the neutrino weak-eigenstate fields $\tilde{\nu}_L^i$ into the mass basis: $\nu_L^i = U^{ij} \tilde{\nu}_L^j$. Applying these transformations, the pertinent parts of the Lagrangian can be written

$$\begin{aligned} \mathcal{L}_\phi &\supset x_{ij} \tilde{\nu}_L^i d_L^j \phi^\dagger - [\mathbf{xV}^\dagger]_{ij} e_L^i u_L^j \phi^\dagger + y_{ij} e_R^i u_R^j \phi + \text{h.c.} \\ &\equiv x_{ij} \tilde{\nu}_L^i d_L^j \phi^\dagger - z_{ij} e_L^i u_L^j \phi^\dagger + y_{ij} e_R^i u_R^j \phi + \text{h.c.} \end{aligned} \quad (2.3)$$

where the Yukawa couplings to the left-handed fermions are related through

$$\mathbf{z} = \mathbf{xV}^\dagger. \quad (2.4)$$

³This can be achieved through the imposition of an appropriate symmetry.

⁴The correspondence between our Yukawa couplings and those of Ref. [40] is $\hat{x}_{ij} = -\lambda_{ji}^L$ and $\hat{y}_{ij} = \lambda_{ji}^{R*}$.

The x_{ij} and y_{ij} are free parameters in our model, with the z_{ij} fixed through Eq. (2.4). The Yukawa couplings of the leptoquark to the first generation of SM fermions are heavily constrained by a number of processes we discuss in Section 3.2. In general, constraints from processes involving the down-quark are more severe for this leptoquark, and for the sake of simplicity we therefore take

$$\mathbf{x} = \begin{pmatrix} 0 & 0 & 0 \\ 0 & x_{22} & x_{23} \\ 0 & x_{32} & x_{33} \end{pmatrix} \quad (2.5)$$

throughout this work. Note that in our notation $x_{22} = x_{\nu_\mu s}$, *et cetera*. We emphasize that even with such a texture, non-zero Yukawa couplings to the up-quark cannot be avoided since they are generated through the quark mixing of Eq. (2.4).

Approximate bounds on the mass of the ϕ can be inferred from collider searches. After pair-production, the final states of interest for this work are $\ell\ell jj$, $\ell jj + \cancel{E}_T$ and $jj + \cancel{E}_T$, where $\ell \in \{\mu, \tau\}$. The current most stringent results from these channels are presented here. Experimental limits are usually presented in (m_{LQ}, β) space, where β represents the branching ratio to the charged lepton and quark. The CMS collaboration places an upper limit of 1080 (760) GeV on the mass of second generation scalar leptoquarks in the $\mu\mu jj$ channel assuming $\beta = 1$ (0.5), while in the combined $\mu\mu jj$ and $\mu jj + \cancel{E}_T$ channel, the mass exclusion reach for $\beta < 1$ is improved: for $\beta = 0.5$, for example, second generation leptoquark masses below 800 GeV are excluded [78]. The most stringent limits in the $bb + \cancel{E}_T$ channel come from ATLAS. Their analysis excludes third generation leptoquark masses below 625 GeV at 95% confidence for $\beta = 0$ [79]. Ref. [80] finds a lower bound between 400 – 640 GeV for the BN leptoquark, although this range is specific to certain parameter choices.

3 Phenomenological analysis

The leptoquark ϕ supports a rich beyond-the-standard-model phenomenology which includes FCNC interactions as well as the possibility of lepton flavor violation and non-universality. The primary motivations for this work are charged current processes in the up-quark sector and FCNCs in the down-quark sector, since these are posited to explain the anomalous measurements in $R_{D^{(*)}}$ and the $b \rightarrow s$ transition, respectively. The new physics essential to explain these anomalies also implies many heavily constrained exotic processes, whose adverse effects on the parameter space available to the model are also computed. Throughout this section, we account for the running of α_s from the leptoquark-mass scale to the scale appropriate to the process considered.

For notational convenience, we remove the breve from the neutrino flavor-eigenstate fields, since we work exclusively with these in this section. We also define

$$\hat{m}_\phi = \frac{m_\phi}{\text{TeV}}. \quad (3.1)$$

3.1 Signals

Below we study the ways in which the leptoquark can ameliorate the discrepancies in the charged current processes $\bar{B} \rightarrow D\tau\bar{\nu}$ and $\bar{B} \rightarrow D^*\tau\bar{\nu}$ as well as the neutral current decays

associated with the anomalous $b \rightarrow s$ data. We also include the leptoquark's contribution to the anomalous magnetic moment of the muon.

3.1.1 Charged current processes

The leptoquark's role in decays of the form $b \rightarrow c \ell_i \nu_j$ can be parameterized by the effective Lagrangian [30]

$$\begin{aligned} \mathcal{L}_{\text{CC}}^{ij} = & -\frac{4G_F}{\sqrt{2}} V_{cb} \left[C_V^{ij} (\bar{c} \gamma^\mu P_L b) (\bar{\ell}_i \gamma_\mu P_L \nu_j) + C_S^{ij} (\bar{c} P_L b) (\bar{\ell}_i P_L \nu_j) \right. \\ & \left. + C_T^{ij} (\bar{c} \sigma^{\mu\nu} P_L b) (\bar{\ell}_i \sigma_{\mu\nu} P_L \nu_j) \right] + \text{h.c.}, \end{aligned} \quad (3.2)$$

with the vector, scalar and tensor contributions generated after Fierz transformation, with Wilson coefficients at the leptoquark mass scale given by

$$C_V^{ij} = \frac{1}{2\sqrt{2}G_F V_{cb}} \frac{z_{i2}^* x_{j3}}{2m_\phi^2} + \delta_{ij}, \quad (3.3a)$$

$$C_S^{ij} = \frac{1}{2\sqrt{2}G_F V_{cb}} \frac{y_{i2} x_{j3}}{2m_\phi^2}, \quad (3.3b)$$

$$C_T^{ij} = -\frac{1}{4} C_S^{ij}. \quad (3.3c)$$

The values of these operators required for a good fit to the available R_D and R_{D^*} data have been studied in the literature, e.g. [30–35], often under the assumption of lepton-flavor conservation—that is, new physics allowed only in $C_{V,S,T}^{33}$. One of the best-fit points suggested by Ref. [32]:

$$\frac{z_{32}^* x_{33}}{\hat{m}_\phi^2} \approx 0.35, \quad \frac{y_{32} x_{33}}{\hat{m}_\phi^2} \approx 0, \quad (3.4)$$

is compatible with new physics only in C_V^{33} , and this is the benchmark considered in the original conception of the BN model. The most recent measurements of R_{D^*} [27, 28] could not have been included in their analysis.

We use these results to guide our study but proceed more generally. We evaluate R_D and R_{D^*} by taking an incoherent sum over neutrino flavors in the final state while accounting for the interference between the SM and leptoquark contributions when the flavors of the charged lepton and neutrino coincide. The ratio R_D is evaluated using recently calculated form factors from lattice QCD [37], and R_{D^*} using form factors [36] extracted from experiments by BaBar [81, 82] and Belle [83, 84], since the lattice results are as yet unavailable. We stress that the $B \rightarrow D^*$ form factors are extracted from measurements of the decays $\bar{B} \rightarrow D^*(\mu, e)\nu$ assuming the SM, and therefore our calculation becomes unreliable when the leptoquark effects in the muonic mode are large. We implement the calculation presented in Ref. [31] and refer the reader there for further detail.

We account for the effects of the running of the strong coupling α_s down from the high scale (Λ) to the b -quark mass scale (μ_b) for the scalar and tensor currents. The vector coefficient C_V does not run due to the Ward identity of QCD. At leading logarithmic order

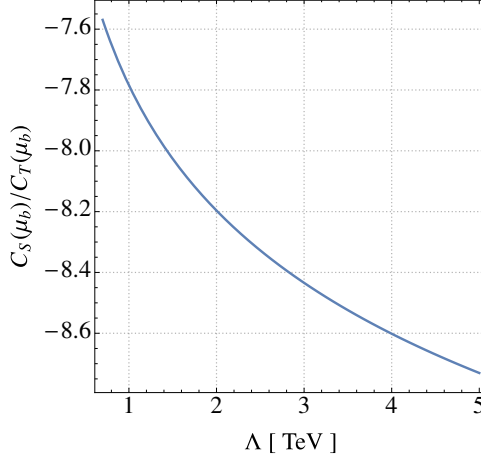


Figure 1: The dependence of the ratio of the tensor and scalar Wilson coefficients evaluated at μ_b in $b \rightarrow c\ell\nu$ as a function of the new-physics scale Λ , at which the ratio is -4 . The figure depicts the values down to which the ratio C_S/C_T evolves at μ_b . For example, running from 1 TeV to μ_b implies $C_S/C_T = -7.8$.

$$C_S(\mu_b) = \left[\frac{\alpha_s(m_t)}{\alpha_s(\mu_b)} \right]^{\frac{\gamma_S}{2\beta_0^{(5)}}} \left[\frac{\alpha_s(\Lambda)}{\alpha_s(m_t)} \right]^{\frac{\gamma_S}{2\beta_0^{(6)}}} C_S(\Lambda), \quad (3.5a)$$

$$C_T(\mu_b) = \left[\frac{\alpha_s(m_t)}{\alpha_s(\mu_b)} \right]^{\frac{\gamma_T}{2\beta_0^{(5)}}} \left[\frac{\alpha_s(\Lambda)}{\alpha_s(m_t)} \right]^{\frac{\gamma_T}{2\beta_0^{(6)}}} C_T(\Lambda), \quad (3.5b)$$

where $\gamma_S = -8$, $\gamma_T = 8/3$ and $\beta_0^{(n_f)} = 11 - 2n_f/3$ [85]. We use the *Mathematica* package *RunDec* [86] to run α_s from $\Lambda \sim \text{TeV}$ to $\mu_b = \overline{m_b} = 4.2 \text{ GeV}$. This results in a modification of the relation between the scalar and tensor Wilson coefficients: $C_T(\Lambda) = -\frac{1}{4}C_S(\Lambda)$. Although most of the running occurs at the low scale (between μ_b and m_t), the relationship between these coefficients still depends non-negligibly on the chosen high scale. To illustrate this dependence, we plot the ratio $C_S(\mu_b)/C_T(\mu_b)$ against Λ in Fig. 1. Running down to μ_b from higher scales increases the magnitude of the scalar coefficient relative to the tensor one.

In Fig. 2 we present the results of our χ^2 fit to the measured values of R_D and R_{D^*} in $C_V^{33}-C_S^{33}$ space to elucidate the regions of interest. Our fit includes experimental uncertainties, but none from the theory side. We fit to our own experimental average: 0.311 ± 0.016 (an error-weighted mean calculated by adding statistical and systematic uncertainties in quadrature) which includes the most recent Belle measurements. For simplicity we assume that the phase of the operators is aligned with the SM contribution and we do not account for the experimental correlation between the measurements of R_D and R_{D^*} . There exist four regions which provide a good fit to the data for $\Lambda = 1 \text{ TeV}$, the most easily accessible has best-fit point $(C_V^{33}, C_S^{33}) \approx (0.11, 0.034)$, corresponding to the same region as that surrounding the point given in Eq. (3.4). Our results in this region are thus in good agreement with those of Ref. [32]. The best-fit points of the four regions are summarized in Table 2.

Region	best-fit point (C_V^{33}, C_S^{33})
A	(0.11, 0.034)
B	(-2.25, 0.81)
C	(-2.12, -0.015)
D	(0.26, -0.81)

Table 2: The best-fit points for our χ^2 fit to the $b \rightarrow c\tau\nu$ data for $\Lambda = 1$ TeV. Four distinct regions emerge from our analysis, of which region *A* is the most convenient to attain in a UV complete model, since it involves small values of the Wilson coefficients and guarantees perturbative Yukawa couplings.

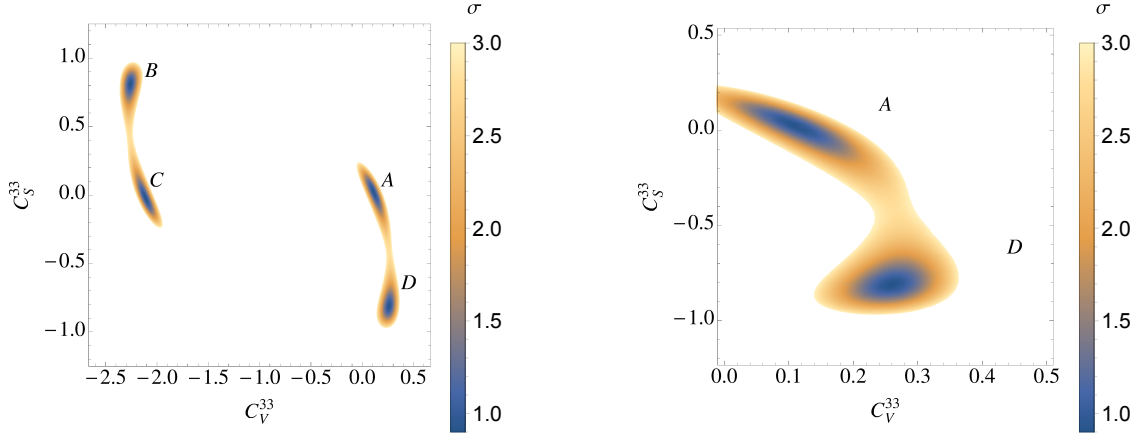


Figure 2: The values for C_V^{33} and C_S^{33} corresponding to a good fit to the R_D and R_{D^*} data at $\Lambda = 1$ TeV. The colors indicate the σ values of our fit. The right plot is zoomed to the area around regions *A* and *D*.

3.1.2 Neutral current processes

The physics underlying the neutral current $b \rightarrow s$ transitions in the model can be described by the effective Lagrangian \mathcal{L}_{NC} :

$$\mathcal{L}_{\text{NC}} = \frac{4G_F}{\sqrt{2}} V_{tb} V_{ts}^* \frac{\alpha}{4\pi} \sum_{IJ} C_{IJ}^\mu \mathcal{O}_{IJ}^\mu, \quad (3.6)$$

where $I, J \in \{L, R\}$ and the operators in this chiral basis are defined below in terms of $\mathcal{O}_{9,10}$. Following the matching procedure performed in Ref. [87], we find that the field ϕ generates the operators

$$\begin{aligned} \mathcal{O}_{LL}^\mu &\equiv \frac{1}{2}(\mathcal{O}_9^\mu - \mathcal{O}_{10}^\mu) = (\bar{s}\gamma^\mu P_L b)(\bar{\mu}\gamma_\mu P_L \mu), \\ \mathcal{O}_{LR}^\mu &\equiv \frac{1}{2}(\mathcal{O}_9^\mu + \mathcal{O}_{10}^\mu) = (\bar{s}\gamma^\mu P_L b)(\bar{\mu}\gamma_\mu P_R \mu) \end{aligned} \quad (3.7)$$

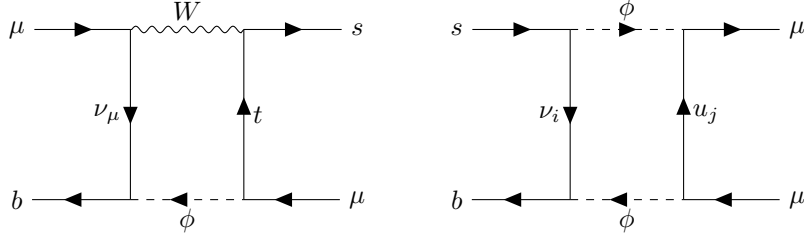


Figure 3: The box diagrams contributing to C_{LL}^ϕ and C_{LR}^ϕ in this scalar leptoquark model.

at the one-loop level with coefficients [40]

$$C_{LL}^{\phi,\mu} = \frac{m_t^2}{8\pi\alpha m_\phi^2} |z_{23}|^2 - \frac{\sqrt{2}}{64\pi\alpha G_F m_\phi^2 V_{tb} V_{ts}^*} \sum_i x_{i3} x_{i2}^* \sum_j |z_{2j}|^2, \quad (3.8a)$$

$$C_{LR}^{\phi,\mu} = \frac{m_t^2}{16\pi\alpha m_\phi^2} |y_{23}|^2 \left[\ln \frac{m_\phi^2}{m_t^2} - f\left(\frac{m_t^2}{m_W^2}\right) \right] - \frac{\sqrt{2}}{64\pi\alpha G_F m_\phi^2 V_{tb} V_{ts}^*} \sum_i x_{i3} x_{i2}^* \sum_j |y_{2j}|^2, \quad (3.8b)$$

where

$$f(x) = 1 - \frac{3}{x-1} + \frac{3}{(x-1)^2} \ln x. \quad (3.9)$$

For the rest of the discussion we remove the μ superscript from the Wilson coefficients and operators associated with $b \rightarrow s\mu\mu$, since we only consider new-physics effects in the muonic mode. The dominant contributions are from the box diagrams shown in Fig. 3. There are additional lepton flavor universal contributions from γ and Z penguins, however these are subdominant: the Z penguins are suppressed by small neutrino masses and only the small short-range contribution from the γ penguins contributes to C_9^ϕ .

The authors of Refs. [2, 16–19] conduct a global fit of all available experimental data on the $b \rightarrow s$ decays. They find a good fit to the data for the chiral coefficients generated by the leptoquark for

$$C_{LL}^{\text{NP}} \approx -1.2 \quad \text{and} \quad C_{IJ}^{\text{NP}} \approx 0 \quad \text{otherwise}, \quad (3.10)$$

where new physics is assumed to significantly alter only the muonic mode and the fit is performed for $C_{IJ} \in \mathbb{R}$. This choice of coefficients eliminates the tensions in $R_{K^{(*)}}$ and results in a significantly improved fit to all of the $b \rightarrow s$ data, with a total 4.2σ pull from the SM [16]. Although a better fit to all of the data can be achieved for $C_{LR}^{\text{NP}} < 0$, the choice $C_{LR}^{\text{NP}} \approx 0$ allows slightly smaller values of C_{LL}^{NP} to explain the $R_{K^{(*)}}$ anomalies. We translate the top plot of Fig. 1 in Ref. [16] into the chiral basis relevant for our leptoquark in Fig. 4 to elucidate the regions of interest. A good fit to the measurements of the LFU observables R_K and R_{K^*} is implied for $-1.8 \lesssim C_{LL}^\phi \lesssim -0.8$ with $C_{LR}^\phi = 0$ and values close to unity for the mixed-chirality contribution require smaller values for C_{LL}^ϕ to meet the central value of the LFU measurements. The condition $C_{LR}^\phi \approx 0$ implies a suppression of the Yukawa

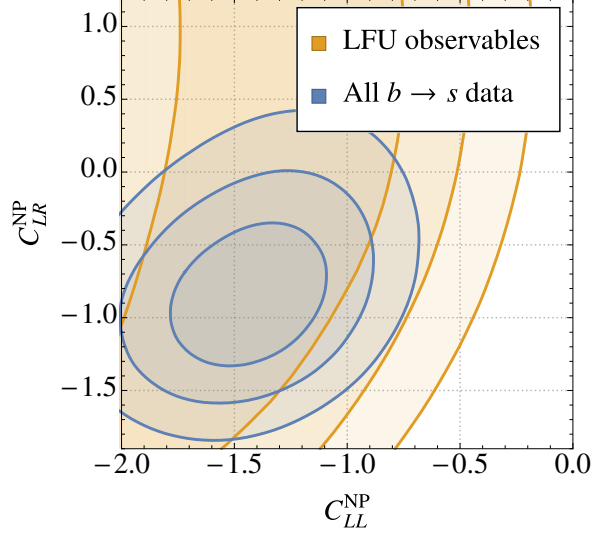


Figure 4: Fig. 1 in Ref. [16] translated into the chiral basis. The figure shows the allowed 1, 2 and 3 σ contours in the $C_{LL}^{\text{NP}}-C_{LR}^{\text{NP}}$ plane. The orange contours represent the fit to only LFU observables while the blue contours take into account all $b \rightarrow s$ observables including the branching ratios of $B_s \rightarrow \mu^+\mu^-$ and the BaBar measurement of $B \rightarrow X_s e^+e^-$ [88].

couplings y_{2i} , while $C_{LL}^\phi \approx -1.2$ requires large leptoquark couplings to the second and third generation of left-handed quarks for the second term in Eq. (3.8a)—corresponding to the second diagram in Fig. 3—to dominate over the first, since it alone can be negative.

Throughout the text, we follow Ref. [41] for the calculation of R_K .

3.1.3 Anomalous magnetic moment of the muon

The leptoquark also mediates one-loop corrections to the $\gamma\mu\mu$ vertex, contributing to the muon anomalous magnetic moment. In the limit that $m_\phi^2 \gg m_t^2$, the contribution of ϕ to $a_\mu = (g-2)_\mu/2$ is given by [40, 89–91]

$$a_\mu^\phi = \sum_i \frac{m_\mu m_{u_i}}{4\pi^2 m_\phi^2} \left(\frac{7}{4} - \ln \frac{m_\phi^2}{m_{u_i}^2} \right) \text{Re}(y_{2i} z_{2i}) - \frac{m_\mu^2}{32\pi^2 m_\phi^2} \left[\sum_i |z_{2i}|^2 + \sum_i |y_{2i}|^2 \right], \quad (3.11)$$

and the same-chirality terms are suppressed relative to the mixed-chirality term by a factor of the muon mass, leading to the requirement of non-vanishing right-handed couplings for an adequate explanation. We require that the leptoquark contribution account for the measured anomaly, and thus that $a_\mu^\phi = (287 \pm 80) \cdot 10^{-11}$ [92].

The top-mass enhancement in the first term makes this the dominant contribution in this model, and we illustrate the interesting values of y_{32} and z_{32} in Fig. 5 for leptoquark mass values of $m_\phi = 1$ TeV and $m_\phi = 5$ TeV. Large z_{23} values assist the model’s explanation of $R_{K^{(*)}}$, hence a combined explanation of this and the $(g-2)_\mu$ anomaly prefers a small y_{23} . Explicitly, the condition [40]

$$-20.7(1 + 1.06 \ln \hat{m}_\phi) \text{Re}(y_{23} z_{23}) \approx 0.08 \hat{m}_\phi^2 \quad (3.12)$$

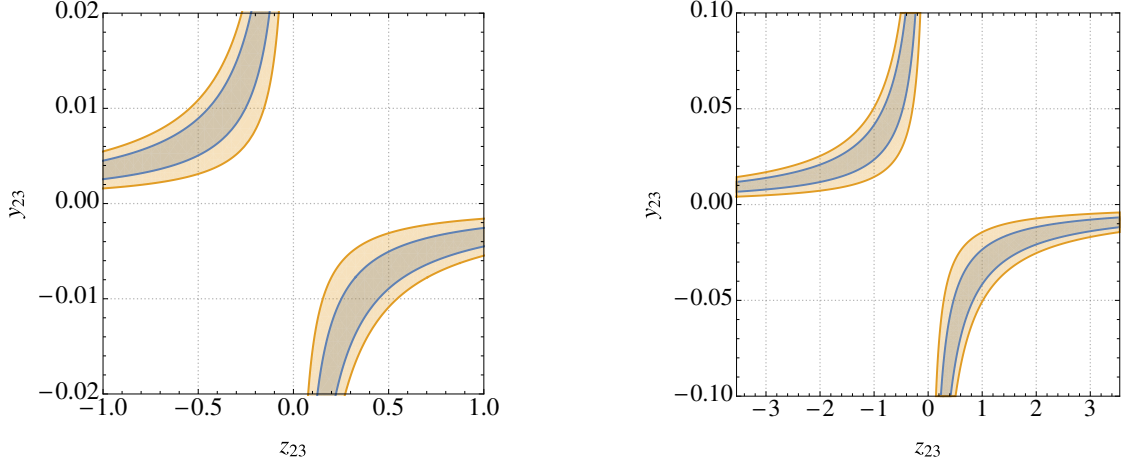


Figure 5: The 1 and 2σ allowed regions for a_μ in the y_{23} – z_{23} plane for leptoquark masses of $m_\phi = 1$ TeV (left) and $m_\phi = 5$ TeV (right). The top-mass enhancement in the first term of Eq. (3.11) allows the model to accommodate a_μ with very small values for $|y_{23}|$ with $z_{23} \neq 0$.

must be satisfied to meet the central value of the measurements of a_μ in this minimal case.

3.2 Constraints

We proceed by studying the constraints important for the leptoquark ϕ in the regions of parameter space dictated by the flavor anomalies. This analysis includes the constraints imposed by B , K and D meson decays, B_s – \bar{B}_s mixing, lepton-flavor violating processes and electroweak measurements.

Many of these processes are studied in the context of an effective-operator framework. Since much of the nomenclature for four-fermion operator coefficients is often only based on the Lorentz-structure of each term, keeping the naming conventions present in the flavor-physics literature for each process can lead to ambiguity. For this reason we index each effective Lagrangian appearing in this section and retain the common names for each term, with the Lagrangian’s index prepended to the label. For example, C_{i,V_L} might correspond to the coefficient of an operator like $(\bar{\phi}\gamma_\mu P_L\chi)(\bar{\psi}\gamma^\mu P_L\omega)$ in \mathcal{L}_i , where ϕ, χ, ψ, ω represent Fermion fields. For clarity we remind the reader that the coefficients of \mathcal{L}_{CC} and \mathcal{L}_{NC} from the previous section are left unindexed.

For the reader’s convenience, we signpost the important results of this section below.

Constraints on the left-handed couplings. A feature of the BN model is that the effective operators mediating the $b \rightarrow s\mu\mu$ decays are generated through box diagrams, since ϕ only couples down-type quarks to neutrinos at tree-level. As a consequence, the large Yukawa couplings required to meet the $b \rightarrow s$ measurements will mediate FCNC processes with a neutrino pair in the final state—processes to which they are related by $SU(2)_L$ invariance—at tree level. This makes the $b \rightarrow s\nu\nu$ decays and $K^+ \rightarrow \pi^+\nu\nu$ very

constraining for this model's explanation of $R_{K^{(*)}}$. The former decay is more important, since it involves the combination of left-handed couplings present in Eq. (3.8): $\sum_i x_{i3} x_{i2}^*$, and essential to ensure a negative value for C_{LL}^ϕ . The leptoquark also contributes to B_s – \bar{B}_s mixing through box diagrams similar to those given in Fig. 3 with neutrinos running through both internal fermion lines. We find measurements of B_s – \bar{B}_s mixing to be more constraining than those of FCNC decays for leptoquark masses larger than a few TeV. For small leptoquark masses, precision electroweak measurements of the $Z\ell\bar{\ell}$ couplings place upper bounds on the sum of the absolute squares of left-handed couplings, and a relative sign difference between couplings to the third-generation quarks and those to the second implies the possibility of a mild cancellation taming these effects. A very important constraint on the left-handed coupling $|x_{22}|$ can be derived from the meson decay $D^0 \rightarrow \mu\mu$, a large value of which aids the explanation of $R_{K^{(*)}}$ in this scenario. It has also recently been pointed out [41] that the LFU evident in the ratio $R_D^{\mu/e} = \Gamma(\bar{B} \rightarrow D\mu\bar{\nu})/\Gamma(\bar{B} \rightarrow De\bar{\nu})$ represents a significant hurdle to the leptoquark's explanation of R_K , and we discuss this constraint below.

Constraints on the product of left-handed couplings discussed above also frustrate the model's attempts to explain measurements of the ratios R_D and R_{D^*} , specifically in those areas of parameter space suggested by new-physics effects only in C_V^{ij} . This implies the need for non-vanishing right-handed couplings y_{ij} .

Constraints on the right-handed couplings. The right-handed couplings y_{ij} are generally less constrained in this leptoquark model, since they mediate interactions involving fewer fermion species. The most stringent limits come from mixed-chirality contributions to tau decays such as $\tau \rightarrow \mu\mu\mu$ and $\tau \rightarrow \mu\gamma$, as well as the precision electroweak measurements mentioned above. Many right-handed couplings also feature in the model's contributions to B , D , and K decays.

3.2.1 Semileptonic charged current processes

Leptonic and semileptonic charged current processes are a sensitive probe of the model we study, since the leptoquark ϕ provides tree-level channels for leptonic pseudoscalar meson decays and semileptonic decays of the tau. In order to describe these processes, we generalize the Lagrangian presented in Eq. (3.2) to

$$\begin{aligned} \mathcal{L}_1^{ijkl} = & -\frac{4G_F}{\sqrt{2}} V_{u_i d_j} \left[C_{1,V}^{ijkl} (\bar{u}_i \gamma^\mu P_L d_j) (\bar{\ell}_k \gamma_\mu P_L \nu_l) + C_{1,S}^{ijkl} (\bar{u}_i P_L d_j) (\bar{\ell}_k P_L \nu_l) \right. \\ & \left. + C_{1,T}^{ijkl} (\bar{u}_i \sigma^{\mu\nu} P_L d_j) (\bar{\ell}_k \sigma_{\mu\nu} P_L \nu_l) \right], \end{aligned} \quad (3.13)$$

where the vector, scalar and tensor Wilson coefficients at the leptoquark mass scale now read

$$C_{1,V}^{ijkl} = \frac{1}{2\sqrt{2}G_F V_{u_i d_j}} \frac{z_{kj}^* x_{li}}{2m_\phi^2} + \delta_{kl}, \quad (3.14a)$$

$$C_{1,S}^{ijkl} = \frac{1}{2\sqrt{2}G_F V_{u_i d_j}} \frac{y_{kj} x_{li}}{2m_\phi^2}, \quad (3.14b)$$

$$C_{1,T}^{ijkl} = -\frac{1}{4} C_{1,S}^{ijkl}, \quad (3.14c)$$

in analogy with Eqs. (3.3). The leptonic decay rate for a pseudoscalar meson $P_{ij} \sim \bar{u}_i d_j$ is then given by [41]

$$\begin{aligned} \Gamma(P_{ij} \rightarrow \ell_k \nu_l) &= \frac{G_F^2 m_P |V_{u_i d_j}|^2}{8\pi} f_P^2 m_{\ell_k}^2 \left(1 - \frac{m_{\ell_l}^2}{m_P^2}\right)^2 \\ &\cdot \left| C_{1,V}^{ijkl} - C_{1,S}^{ijkl} \frac{m_P^2}{m_{\ell_k}(m_{u_i} + m_{d_j})} \right|^2, \end{aligned} \quad (3.15)$$

where f_P is the pseudoscalar meson decay constant. As before, we account for the effect of the running of α_s from the high scale to the scales appropriate for each decay for the scalar operator. We take the relevant scale to be $\mu = \bar{m}_c = 1.27$ GeV for the D meson decays and $\mu = 2$ GeV for the K decays, since this is the matching scale used in Ref. [93], from which we take the decay constants. Explicitly,

$$C_{1,S}(\mu) = \left[\frac{\alpha_s(m_b)}{\alpha_s(\mu)} \right]^{\frac{\gamma_S}{2\beta_0^{(4)}}} \left[\frac{\alpha_s(m_t)}{\alpha_s(m_b)} \right]^{\frac{\gamma_S}{2\beta_0^{(5)}}} \left[\frac{\alpha_s(\Lambda)}{\alpha_s(m_t)} \right]^{\frac{\gamma_S}{2\beta_0^{(6)}}} C_{1,S}(\Lambda), \quad (3.16)$$

while the running for the scalar operator featuring in the B decays is the same as in Eq. (3.5). Eq. (3.15) is finely sensitive to the Wilson coefficient $C_{1,S}$ since it has the effect of lifting the chiral suppression of the SM due to the charged lepton mass in the denominator of the last term. Recent work [41] has pointed out the importance of considering the decays $B \rightarrow \ell \bar{\nu}$, $K \rightarrow \ell \bar{\nu}$, $D_s \rightarrow \ell \bar{\nu}$ and $B \rightarrow D^{(*)} \ell \nu$, to which we also add a discussion of $\tau \rightarrow K \nu$ and $B_c \rightarrow \ell \bar{\nu}$ below. In addition, for each relevant process we calculate a LFU ratio, since in many cases these are well measured quantities which constitute powerful probes of any new-physics attempting to explain $R_{D^{(*)}}$ or $R_{K^{(*)}}$. We summarize the limits and values we take for these decays and their relevant ratios in Table 3. All values of the decay constants used throughout this discussion are taken from Ref. [93].

The ratio

$$r_K^{e/\mu} = \frac{\Gamma(K \rightarrow e \nu)}{\Gamma(K \rightarrow \mu \nu)} \quad (3.17)$$

is one of the most precisely measured quantities in weak hadronic physics. As such, the consideration of next-to-leading-order corrections becomes important for our phenomenological analysis of the effects of the leptoquark ϕ on these decays. Electroweak effects contributing to $r_K^{e/\mu}$ have been calculated to order $e^2 p^4$ in chiral perturbation theory, e.g. [99, 100]. Higher order contributions to the quotient Eq. (3.17) are proportional to the lowest order

Observable	Experimental value
$\text{Br}(K \rightarrow \mu\nu)$	$(63.56 \pm 0.11)\%$
$\text{Br}(D_s \rightarrow \mu\nu)$	$(0.556 \pm 0.025)\%$
$\text{Br}(D_s \rightarrow \tau\nu)$	$(5.55 \pm 0.24)\%$
$\text{Br}(B \rightarrow \mu\nu)$	$< 1.0 \cdot 10^{-6}$
$\text{Br}(B \rightarrow \tau\nu)$	$(1.09 \pm 0.24) \cdot 10^{-4}$
$\text{Br}(B_c \rightarrow \tau\nu)$	$\lesssim 30\%$ [94]
$r_K^{e/\mu} = \frac{\Gamma(K \rightarrow e\nu)}{\Gamma(K \rightarrow \mu\nu)}$	$(2.488 \pm 0.009) \cdot 10^{-5}$
$R_K^{\tau/\mu} = \frac{\Gamma(\tau \rightarrow K\nu)}{\Gamma(K \rightarrow \mu\nu)}$	$(1.101 \pm 0.016) \cdot 10^{-2}$
$R_{D_s}^{\tau/\mu} = \frac{\Gamma(D_s \rightarrow \tau\nu)}{\Gamma(D_s \rightarrow \mu\nu)}$	$10.73 \pm 0.69^{+0.56}_{-0.53}$ [95]
$R_D^{\mu/e} = \frac{\Gamma(B \rightarrow D\mu\nu)}{\Gamma(B \rightarrow De\nu)}$	$0.995 \pm 0.022 \pm 0.039$ [96]
$R_{D^*}^{e/\mu} = \frac{\Gamma(B \rightarrow D^*e\nu)}{\Gamma(B \rightarrow D^*\mu\nu)}$	$1.04 \pm 0.05 \pm 0.01$ [97]

Table 3: A table summarizing the experimental values we take for the various leptonic branching ratios and LFU ratios considered in this section. Measurements quoted without explicit citation are taken from Ref. [98].

contribution: $r_K^{e/\mu,(0)}$, calculated directly from Eq. (3.15). Including the effects of leading higher-order logarithms through Δ_{LL} , Eq. (3.17) can be written

$$r_K^{e/\mu} = r_K^{e/\mu,(0)} \left(1 + \Delta_{e^2 p^2}^K + \Delta_{e^2 p^4}^K + \dots \right) (1 + \Delta_{LL}) \quad (3.18)$$

and we take $\Delta_{LL} = 0.055\%$, $\Delta_{e^2 p^2}^K = -3.786\%$ and $\Delta_{e^2 p^4}^K = (0.135 \pm 0.011)\%$ [99] in our calculation.

One can extend the study of lepton-flavor universality in leptonic kaon decays by considering the crossed process $\tau \rightarrow K\nu$. More specifically, the ratio

$$R_K^{\tau/\mu} = \frac{\Gamma(\tau \rightarrow K\nu)}{\Gamma(K \rightarrow \mu\nu)} \quad (3.19)$$

can be used to derive constraints on the muon and tau couplings of the leptoquark ϕ , and a similar approach has been taken to constrain the couplings of a vector leptoquark in Ref. [49]. For the numerator, we find

$$\Gamma(\tau \rightarrow K\nu) = \frac{G_F^2 |V_{us}|^2}{8\pi} f_K^2 m_\tau^3 \left(1 - \frac{m_K^2}{m_\tau^2} \right)^2 \sum_i \left| C_{1,V}^{123i} - C_{1,S}^{123i} \frac{m_K^2}{m_\tau(m_u + m_s)} \right|^2, \quad (3.20)$$

and the ratio $R_K^{\tau/\mu}$ is required to lie within 2σ of its experimental value: $(1.101 \pm 0.016) \cdot 10^{-2}$ [98].

Pion leptonic decays have been well-studied in the context of leptoquark models, and measurements of the ratio $R_\pi^{\mu/e} = \Gamma(\pi \rightarrow \mu\nu)/\Gamma(\pi \rightarrow e\nu)$ demand that leptoquark interactions with the electron and first-generation quarks are small⁵ [101, 102]. The electron and

⁵In the most minimal case, a non-zero x_{21} implies $z_{21} \approx x_{21}$ and these couplings alone are sufficient to mediate the decay $\pi^+ \rightarrow \mu^+ \nu$.

down-quark couplings play no role in the anomalies we consider in this work, and we only require that the appropriate couplings are small enough to evade these constraints.

Comments on lepton flavor universality in $B \rightarrow D^{(*)}(e, \mu)\bar{\nu}$. An additional constraint comes from the observation that LFU is respected in the ratio of decay rates

$$R_{D^{(*)}}^{\mu/e} = \frac{\Gamma(\bar{B} \rightarrow D^{(*)}\mu\bar{\nu})}{\Gamma(\bar{B} \rightarrow D^{(*)}e\bar{\nu})}, \quad (3.21)$$

implying a tension with the purported violation in μ - e universality evident in $R_{K^{(*)}}$. This constraint has been studied in Ref. [41], where it was concluded that the leptoquark model cannot respect this constraint while explaining the suppression of R_K in the absence of the right-handed couplings y_{ij} . The ratio has been measured to be $R_D^{\mu/e} = 0.995 \pm 0.022 \pm 0.039$ [96], while the reciprocal is presented for the D^* ratio: $R_{D^*}^{e/\mu} = 1.04 \pm 0.05 \pm 0.01$ [97]. In the case of $R_D^{\mu/e}$, 2σ consistency with the measurement allows for an approximately 10% deviation from the SM prediction, a weaker bound than that presented in Ref. [41], while the recent Belle result for $R_{D^*}^{e/\mu}$ permits only a 4% deviation for contributions to the muonic mode. We find that these constraints become less important for leptoquark masses larger than 1 TeV, permitting sizeable contributions to R_K in this model. We illustrate this point in the top plot of Fig. 6, where random points passing all of the constraints presented in our analysis except $R_{D^*}^{e/\mu}$ are presented in the R_K - $R_D^{\mu/e}$ plane. The parameters and ranges taken in our scan are the same as those of scan I in Sec. 4 in which masses are sampled randomly from the range [1, 5] TeV. The complementary set-up for $R_{D^*}^{e/\mu}$ is shown in the bottom figure of Fig. 6, *mutatis mutandis*.

Comments on $B_c \rightarrow \tau\nu$. The leptonic decays of the charmed B meson have not yet been measured—few B_c mesons are produced at e^+e^- B -factories and the leptonic mode cannot be reliably reconstructed at LHCb. Despite this, measurements of the B_c lifetime have recently been shown to imply serious constraints [94, 103] for models explaining $R_{D^{(*)}}$ with contributions to the operator C_S^{3i} defined in Eq. (3.2). Here, we wish to point out that the $B_c \rightarrow \tau\nu$ rate remains SM-like in this leptoquark model due to the presence of the tensor contribution C_T^{3i} , and thus that measurements of the B_c lifetime do not constitute a serious constraint on the model.

In Fig. 7 we plot the branching ratio $\text{Br}(B_c \rightarrow \tau\nu)$ in this leptoquark model against interesting values of R_{D^*} , in the spirit of Fig. 1 of Ref. [94]. The blue curve represents the contribution from only the Wilson coefficient C_S , while the orange curve represents the contribution from the scalar leptoquark ϕ where the scalar and tensor contributions are related through Eq. (3.14c). The presence of both the scalar and tensor contributions results renders the branching ratio SM-like, or slightly suppressed, in the region of interest.

3.2.2 Lepton flavor violating processes

The lepton-flavor symmetries present in the SM are broken by the Yukawa couplings of the leptoquark to the SM fermions. This implies that ϕ can mediate processes that do not

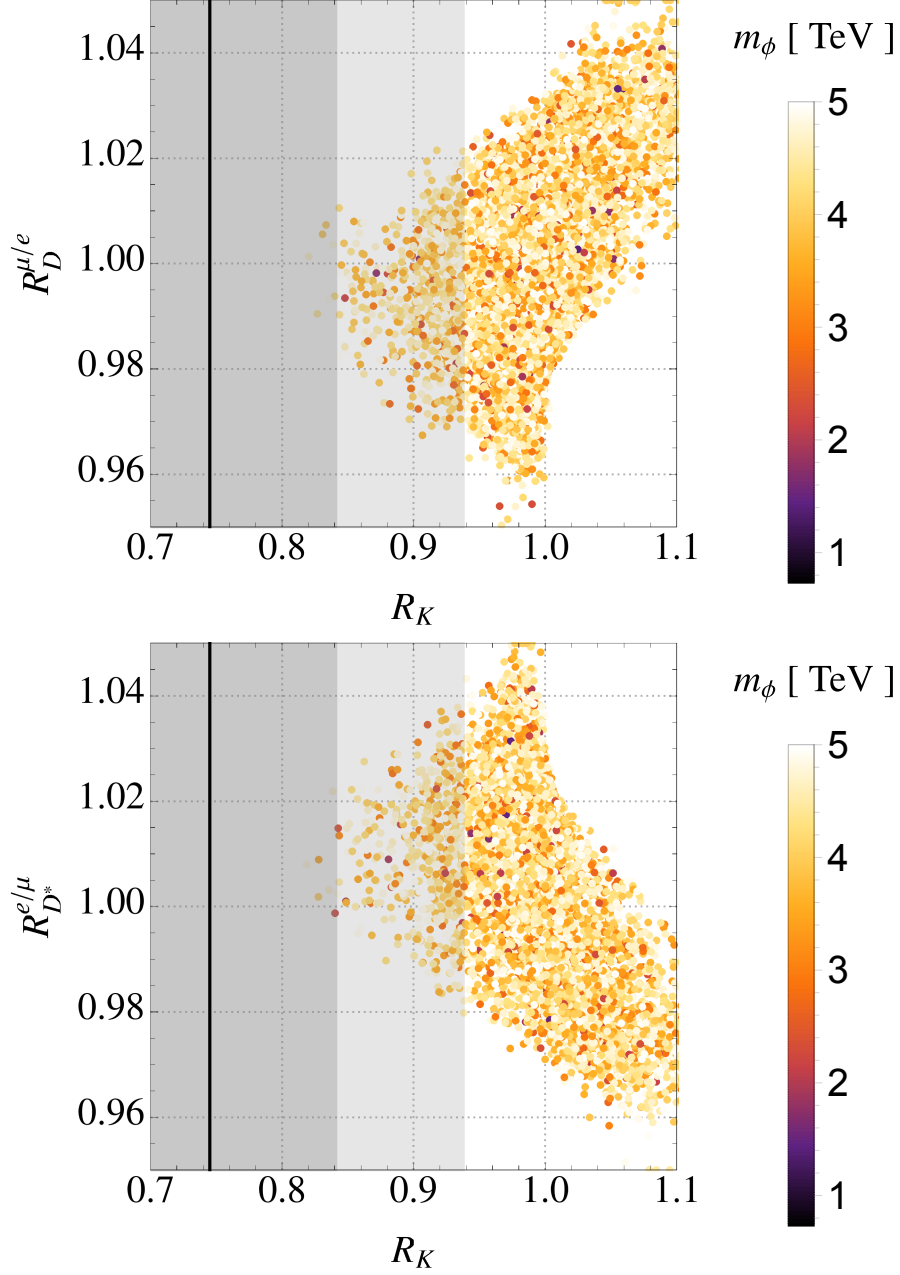


Figure 6: The results of our random scan showing R_K against $R_D^{\mu/e}$ (top) and $R_{D^*}^{e/\mu}$ (bottom) for the parameter choices detailed in Sec. 4 for ‘scan I’, in which the leptoquark mass is allowed to vary to values as large as 5 TeV. For leptoquark masses between 3 and 5 TeV, the tension in R_K can be significantly resolved while keeping LFU effects between electron and muon modes mild.

conserve lepton flavor, of which those considered in our analysis are $\ell_i \rightarrow \ell_j \gamma$, $\ell_i \rightarrow \ell_j \ell_k \ell_l$ and muon–electron conversion in nuclei: $\mu_Z^A \text{N} \rightarrow e_Z^A \text{N}$. We use the expressions for these processes found in the Appendix of Ref. [76], adapted to the case of one leptoquark, and

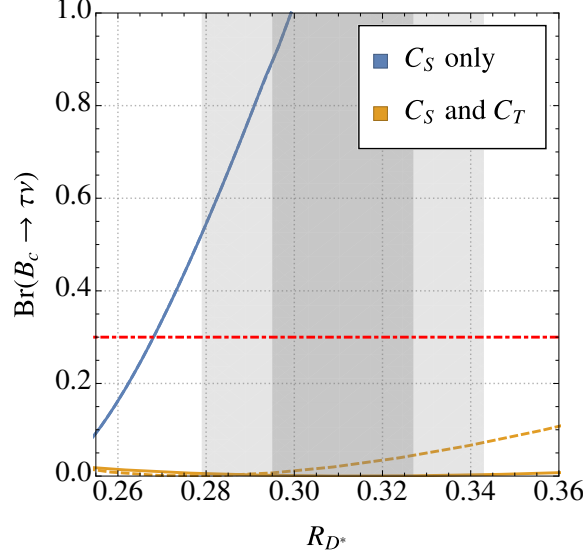


Figure 7: The branching ratio $\text{Br}(B_c \rightarrow \tau \nu)$ against R_{D^*} with new physics only in C_S (solid blue) and new physics in both C_S and C_T satisfying $C_S/C_T = -4$ (solid orange) and $C_S/C_T = -7.8$ (dashed orange). The 30% limit is shown in red (dot-dashed). The dark and light grey regions represent the 1 and 2σ regions for $R_{D^{(*)}}$. In this leptoquark model, $\text{Br}(B_c \rightarrow \tau \nu)$ remains SM-like in the region of interest.

direct the reader there for more details. We impose the following limits for the constraints:

$$\text{Br}(\tau \rightarrow \mu \gamma) < 4.4 \cdot 10^{-8} \quad [104], \quad (3.22)$$

$$\text{Br}(\tau \rightarrow \mu \mu \mu) < 2.1 \cdot 10^{-8} \quad [105], \quad (3.23)$$

$$\text{Br}(\mu^{197}\text{Au} \rightarrow e^{197}\text{Au}) < 7.0 \cdot 10^{-13} \quad [106]. \quad (3.24)$$

In the $\mu \rightarrow e$ transition, we only consider muon–electron conversion since this is the most stringent of the muon’s LFV decay modes that the leptoquark can mediate [74, 76, 107]. The tree-level contributions to muon–electron conversion imply very strong constraints on the coupling combinations involved. Assuming no accidental cancellation between terms, the order-of-magnitude bounds [76]

$$z_{21}y_{11}^*, y_{21}z_{11}^* \lesssim (4 \cdot 10^{-9} - 7 \cdot 10^{-8}) \frac{m_\phi^2}{m_W^2}, \quad (3.25)$$

$$z_{21}z_{11}^*, y_{21}y_{11}^* \lesssim (10^{-8} - 10^{-7}) \frac{m_\phi^2}{m_W^2}. \quad (3.26)$$

can be evaded with small electron couplings.

3.2.3 Rare meson decays

The most important rare meson decays remain to be mentioned. We group them here and separate their discussion based on the species of lepton in the final state. The decays

studied are: (1) $B \rightarrow K\nu\nu$ and $K^+ \rightarrow \pi^+\nu\nu$, involving neutrinos, and (2) $D^0 \rightarrow \mu\mu$ and $D^+ \rightarrow \pi^+\mu\mu$, involving charged leptons.

The decays $B \rightarrow K\nu\nu$ and $K^+ \rightarrow \pi^+\nu\nu$ heavily constrain the combination of Yukawa couplings x_{ij} in this model since the SM contributions proceed at loop-level, while our leptoquark mediates such neutral current quark decays at tree-level. The physics describing this class of decays is described by the effective Lagrangian [108, 109]

$$\begin{aligned} \mathcal{L}_2^{ijkl} = & \frac{8G_F}{\sqrt{2}} \frac{e^2}{16\pi^2} V_{td_i} V_{td_j}^* \left[C_{2,L}^{ijkl} (\bar{d}_i \gamma_\mu P_L d_j) (\bar{\nu}_k \gamma^\mu P_L \nu_l) \right. \\ & \left. + C_{2,R}^{ijkl} (\bar{d}_i \gamma_\mu P_R d_j) (\bar{\nu}_k \gamma^\mu P_L \nu_l) \right] + \text{h.c.} \end{aligned} \quad (3.27)$$

and operator coefficients

$$C_{2,L}^{ijkl} = -\frac{\sqrt{2}\pi^2}{e^2 G_F m_\phi^2} \frac{x_{kj}^* x_{li}}{V_{td_i} V_{td_j}^*} + C_L^{\text{SM}} \delta_{kl}, \quad C_{2,R}^{ijkl} = 0, \quad (3.28)$$

where $C_L^{\text{SM}} = -X(m_t^2/m_W^2)/s_w^2$. The SM loop function $X(x)$ is given by [108–111]

$$X(x) = \frac{x}{8} \left[\frac{x+2}{x-1} + \frac{3x-6}{(x-1)^2} \ln x \right], \quad (3.29)$$

and the ratio $R_K^{\nu\nu} \equiv \Gamma(B \rightarrow K\nu\nu)/\Gamma(B \rightarrow K\nu\nu)_{\text{SM}}$ is constrained to satisfy $R_K^{\nu\nu} < 4.3$ at 90% C.L. [112]. We find

$$\begin{aligned} R_K^{\nu\nu} &= \frac{1}{3} \sum_{ij} \frac{|C_{2,L}^{32ij}|^2}{|C_L^{\text{SM}}|^2} \\ &= 1 + \frac{a^2}{3m_\phi^4} \sum_{ij} \left| \frac{x_{i2}^* x_{j3}}{V_{tb} V_{ts}^*} \right|^2 - \frac{2a}{3m_\phi^2} \sum_i \text{Re} \left(\frac{x_{i2}^* x_{i3}}{V_{tb} V_{ts}^*} \right), \end{aligned} \quad (3.30)$$

where $a = \sqrt{2}\pi^2/(e^2 G_F |C_L^{\text{SM}}|)$. Due to the absence of right-handed currents, our model predicts $R_K^{\nu\nu} = R_{K^*}^{\nu\nu}$ although the bound on $R_{K^*}^{\nu\nu}$ is slightly weaker, as is that for the inclusive decay. A conservative limit on the combination $(\sum x_{i2}^* x_{i3})/\hat{m}_\phi^2$ can be derived using the Schwartz inequality [40]:

$$-0.05 \lesssim \frac{[\mathbf{x}^\dagger \mathbf{x}]_{23}}{\hat{m}_\phi^2} \lesssim 0.1, \quad (3.31)$$

where we have assumed $\text{Arg}(x_{i2}^* x_{i3}) = \text{Arg}(V_{tb} V_{ts}^*)$. We emphasize that this bound represents an insufficient condition for the model to respect the experimental limits. In Fig. 8 we present the allowed region for non-zero x_{32} and x_{33} and $m_\phi = 1$ TeV—a coupling texture interesting for explaining $R_{D^{(*)}}$, although heavily constrained by $R_K^{\nu\nu}$.

The decay $K^+ \rightarrow \pi^+\nu\nu$ constitutes the most stringent constraint on our model from the kaon sector [113]. We find

$$\begin{aligned} \text{Br}(K^+ \rightarrow \pi^+\nu\nu) &= \frac{1}{3} \sum_{ij} \kappa_+ \left[\left(\text{Im} \frac{V_{ts} V_{td}^* s_w^2 C_{2,L}^{21ij}}{\lambda^5} \right)^2 \right. \\ &\quad \left. + \left(\text{Re} \frac{V_{tb} V_{ts}^* s_w^2 C_{2,L}^{21ij}}{\lambda^5} + P_{(u,c)} \delta_{ij} \right)^2 \right], \end{aligned} \quad (3.32)$$

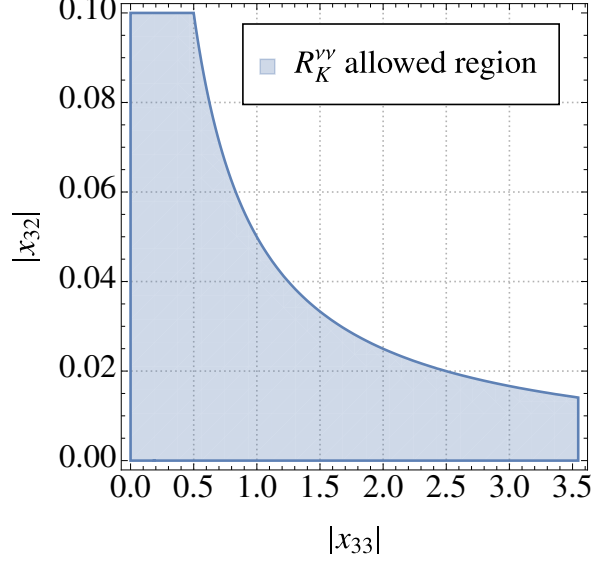


Figure 8: The region allowed by experimental limits on the decay $B \rightarrow K \nu \nu$ in the $|x_{33}|$ – $|x_{32}|$ plane for $m_\phi = 1$ TeV. All other couplings are switched off. A large value of $|x_{33}|$ is essential to explaining $R_{D^{(*)}}$, and the figure implies that such a requirement keeps $|x_{32}|$ small.

by adapting Eq. (3.29) of Ref. [108], where the factor $\kappa_+ = (5.27 \pm 0.03) \cdot 10^{-11}$ is due mainly to hadronic matrix elements, λ is the CKM Wolfenstein parameter, $P_{(u,c)} = 0.41 \pm 0.05$ accounts for the effects of light-quark loops, and the small electromagnetic corrections have been neglected. The branching ratio for the decay has most recently been measured by the E949 collaboration to be $\text{Br}(K^+ \rightarrow \pi^+ \nu \nu) = (1.73_{-1.05}^{+1.15}) \cdot 10^{-10}$ [114]. A conservative limit can be placed on the combination of new-physics couplings featuring in $C_{2,L}^{21ij}$ by considering only same-flavored neutrinos in the final state of the decay. Under the assumptions that the couplings involved are real and that only one combination dominates, we find

$$-9.1 \cdot 10^{-4} < \frac{[\mathbf{x}^\dagger \mathbf{x}]_{21}}{\hat{m}_\phi^2} < 4.8 \cdot 10^{-4}. \quad (3.33)$$

This bound can be avoided by considering a suppression of the leptoquark couplings to the first generation of quarks.

In this leptoquark model, the coupling of the c -quark to the charged leptons is essential for the explanation of the $b \rightarrow c \tau \nu$ anomalies. Also, as discussed earlier, the up-quark couplings cannot be entirely avoided due to the stringency of Eq. (3.33) and the mixing of Eq. (2.4). These factors make the physics of operators of the form $\mathcal{O}_{ijkl} \sim (u_i \Gamma u_j)(\ell_k \Gamma \ell_l)$ an important source of constraint on this model. Additionally, in order to ensure $C_{LL}^\phi \approx -1.2$ in the model’s original conception, an ansatz for z_{ij} was chosen such that $|z_{22}|$ takes $\mathcal{O}(1)$ values. Constraints from the decays $D^0 \rightarrow \mu \mu$ and $D^+ \rightarrow \pi^+ \mu \mu$ are especially worrying in this case, since the leptoquark mediates these processes at tree-level. Even within the context of vanishing first-generation couplings, one cannot avoid inducing new-physics interactions involving up quarks because of the mixing of Eq. (2.4). The new-physics

contributions to decays of the form $u_i \rightarrow u_j \ell_k \ell_l$ can be contained within the effective Lagrangian

$$\begin{aligned} \mathcal{L}_3^{ijkl} = \frac{4G_F}{\sqrt{2}} & \left[C_{3,V_R}^{ijkl} (\bar{u}_i \gamma_\mu P_R u_j) (\bar{\ell}_k \gamma^\mu P_R \ell_l) + C_{3,V_L}^{ijkl} (\bar{u}_i \gamma_\mu P_L u_j) (\bar{\ell}_k \gamma^\mu P_L \ell_l) \right. \\ & + C_{3,T}^{ijkl} (\bar{u}_i \sigma_{\mu\nu} P_R u_j) (\bar{\ell}_k \sigma^{\mu\nu} P_R \ell_l) + C_{3,S_L}^{ijkl} (\bar{u}_i P_L u_j) (\bar{\ell}_k P_L \ell_l) \\ & \left. + C_{3,S_R}^{ijkl} (\bar{u}_i P_R u_j) (\bar{\ell}_k P_R \ell_l) + \text{h.c.} \right], \end{aligned} \quad (3.34)$$

with coefficients $C_{3,i}$ at the leptoquark mass scale given by

$$C_{3,\{V_L, V_R\}}^{ijkl} = \frac{1}{2\sqrt{2}G_F} \left\{ \frac{z_{kj} z_{li}^*}{y_{kj}^* y_{li}} \right\} \frac{1}{2m_\phi^2}, \quad (3.35)$$

$$C_{3,\{S_L, S_R\}}^{ijkl} = \frac{1}{2\sqrt{2}G_F} \left\{ \frac{z_{kj} y_{li}}{y_{kj}^* z_{li}^*} \right\} \frac{1}{2m_\phi^2}, \quad (3.36)$$

$$C_{3,T}^{ijkl} = -\frac{1}{4} C_{3,S_L}^{ijkl}. \quad (3.37)$$

For the scalar and tensor operators we account for the running of α_s down to the charm-quark mass scale as in Sec. 3.2.1.

For the leptonic decay, we find

$$\begin{aligned} \Gamma(D^0 \rightarrow \mu\mu) = \frac{f_D^2 m_D^3 G_F^2}{32\pi} \left(\frac{m_D}{m_c} \right)^2 \beta_\mu & \left[|C_{3,S_L}^{2122} - C_{3,S_R}^{2122}|^2 \beta_\mu^2 \right. \\ & \left. + \left| C_{3,S_L}^{2122} + C_{3,S_R}^{2122} - \frac{2m_\mu m_c}{m_D^2} (C_{3,V_L}^{2122} + C_{3,V_R}^{2122}) \right|^2 \right] \end{aligned} \quad (3.38a)$$

$$\begin{aligned} = \frac{f_D^2 m_D^3}{512\pi m_\phi^4} \left(\frac{m_D}{m_c} \right)^2 \beta_\mu & \left[|y_{22}^* z_{21}^* - z_{22} y_{21}|^2 \beta_\mu^2 \eta^2 \right. \\ & \left. + \left| \eta(y_{22}^* z_{21}^* + z_{22} y_{21}) - \frac{2m_\mu m_c}{m_D^2} (z_{22} z_{21}^* + y_{22}^* y_{21}) \right|^2 \right], \end{aligned} \quad (3.38b)$$

where $\beta_\mu = (1 - 4m_\mu^2/m_D^2)^{1/2} \approx 0.99$, $f_D = 212(2)$ MeV [93] and $\eta = C_{3,S_L}^{2122}(\overline{m_c})/C_{3,S_L}^{2122}(m_\phi)$. In the limit that the left-handed contribution dominates, the bound

$$|x_{22}| < 0.46 \hat{m}_\phi \quad (3.39)$$

can be derived from the experimental upper limit $\text{Br}(D^0 \rightarrow \mu\mu) < 7.6 \cdot 10^{-9}$ [115] assuming $x_{23} \ll x_{22}$. One can arrange for a mild cancellation between the same- and mixed-chirality terms in Eq. (3.38) by allowing the right-handed couplings $y_{2(1,2)}$ to take $\mathcal{O}(0.1)$ values, however this creates tensions with other meson decays such as $D_s \rightarrow \mu\nu$, $K \rightarrow \mu\nu$ and $D^+ \rightarrow \pi^+ \mu\mu$, and we find no overlapping allowed region.

For the decay $D^+ \rightarrow \pi^+ \mu\mu$, we implement the calculation of Ref. [116]. The branching ratio

$$\text{Br}(D^+ \rightarrow \pi^+ \mu^+ \mu^-) < 8.3 \cdot 10^{-8}, \quad (3.40)$$

is measured by extrapolating spectra over the resonant region [117], while the bounds on the separate high- and low- q^2 bins are

$$\text{Br}(D^+ \rightarrow \pi^+ \mu^+ \mu^-)_{q^2 \in [1.56, 4.00]} < 2.9 \cdot 10^{-8}, \quad (3.41)$$

$$\text{Br}(D^+ \rightarrow \pi^+ \mu^+ \mu^-)_{q^2 \in [0.0625, 0.276]} < 2.5 \cdot 10^{-8}, \quad (3.42)$$

where q^2 ranges are given in GeV^2 . Both Eq. (3.41) and Eq. (3.42) are imposed in our numerical scans.

3.2.4 Meson mixing

A complementary constraint on the left-handed couplings can be derived from $B_s - \bar{B}_s$ mixing, providing a stronger bound than $R_K^{\nu\nu}$ for leptoquark masses larger than a few TeV. The *UTfit* collaboration determines constraints on $\Delta F = 2$ processes in terms of the quotient of the meson mixing amplitude and the SM prediction:

$$C_{B_s} e^{2i\phi_{B_s}} \equiv \frac{\langle B_s | \mathcal{H}^{\Delta F=2} | \bar{B}_s \rangle}{\langle B_s | \mathcal{H}_{\text{SM}}^{\Delta F=2} | \bar{B}_s \rangle}, \quad (3.43)$$

and the current best fit values for these parameters are $C_{B_s} = 1.052 \pm 0.084$ and $\phi_{B_s} = (0.72 \pm 2.06)^\circ$ [118]. In the notation of Ref. [118], our leptoquark only generates the effective operator $Q_1^{ij} = C_1^{bs} (\bar{q}_i^\alpha \gamma_\mu P_L q_j^\alpha) (\bar{q}_i^\beta \gamma^\mu P_L q_j^\beta)$, where α and β are color indices, through box diagrams with neutrinos and leptoquarks in the loop. The relevant operator coefficient, defined at the high scale Λ , is

$$C_1^{bs, \phi}(\Lambda) = \frac{1}{128\pi^2} \left(\sum_i \frac{x_{i3}^* x_{i2}}{m_\phi} \right)^2, \quad (3.44)$$

in the limit of vanishing SM fermion masses. The SM processes involve similar box diagrams with top quarks and W bosons in the loop, inducing the Wilson coefficient (see e.g. [119])

$$C_1^{bs, \text{SM}} = \frac{G_F^2 m_W^2}{4\pi^2} (V_{tb}^* V_{ts})^2 S_0(m_t^2/m_W^2), \quad (3.45)$$

where $S_0(x)$ is the well-known Inami-Lim function [120]:

$$S_0(x) = \frac{x^3 - 11x^2 + 4x}{4(x-1)^2} - \frac{3x^3}{2(x-1)^3} \ln x. \quad (3.46)$$

We account for the effect of the running of α_s down to m_W for the coefficient $C_1^{bs, \phi}$ to compare with the SM result using [121]

$$C_1^{bs, \phi}(m_W) = \left[\frac{\alpha_s(m_t)}{\alpha_s(m_W)} \right]^{\frac{\gamma}{2\beta_0^{(5)}}} \left[\frac{\alpha_s(\Lambda)}{\alpha_s(m_t)} \right]^{\frac{\gamma}{2\beta_0^{(6)}}} C_1^{bs, \phi}(\Lambda), \quad (3.47)$$

where $\gamma = 4$ and $\beta_0^{(n_f)} = 11 - 2n_f/3$. The combination of left-handed couplings in Eq. (3.44) is thus required to satisfy

$$C_{B_s} e^{2i\phi_{B_s}} = 1 + \frac{1}{32G_F^2 m_W^2 S_0(m_t^2/m_W^2)} \left(\frac{\eta'}{V_{tb}^* V_{ts}} \sum_i \frac{x_{i3}^* x_{i2}}{m_\phi} \right)^2, \quad (3.48)$$

where $\eta' = C_1^{bs, \phi}(m_W)/C_1^{bs, \phi}(m_\phi)$.

3.2.5 Precision electroweak measurements

The Yukawa interactions of the leptoquark with both left- and right-handed SM fermions give corrections to many electroweak observables. Precision measurements of these have been translated into bounds on dimension-six operators in the literature, and we proceed by applying the results of a recent fit to the electroweak precision data [122]. Specifically, we consider the way in which the couplings x_{ij} and y_{ij} are constrained by precision electroweak measurements of the $Z\ell\bar{\ell}$ couplings g_L and g_R . These receive corrections from leptoquark loops in our model [40]:

$$\begin{aligned} \delta g_I^{\ell_i} = & (-1)^{\delta_{IR}} \frac{3}{32\pi^2} \frac{m_t^2}{m_\phi^2} \left(\ln \frac{m_\phi^2}{m_t^2} - 1 \right) |\lambda_{i3}^I|^2 \\ & - \frac{1}{32\pi^2} \frac{m_Z^2}{m_\phi^2} \sum_j^2 |\lambda_{ij}^I|^2 \left[\left(\delta_{IL} - \frac{4s_w^2}{3} \right) \left(\ln \frac{m_\phi^2}{m_Z^2} + i\pi + \frac{1}{3} \right) - \frac{s_w^2}{9} \right], \end{aligned} \quad (3.49)$$

where $I \in \{L, R\}$, $\lambda_{ij}^L = z_{ij}$ and $\lambda_{ij}^R = y_{ij}$. From Eq. (3.28) and Table 10 of Ref. [122], we calculate the conservative constraints

$$\text{Re} \delta g_L^{\ell_i} \in [-8.5, 12.0] \cdot 10^{-4}, \quad \text{Re} \delta g_R^{\ell_i} \in [-5.4, 6.7] \cdot 10^{-4} \quad (3.50)$$

at 95% confidence from the fit results obtained using the large- m_t expansion. The expressions in Eq. (3.50) are conservative since we do not account for correlations between different operators but this does not affect our results in an important way. The results of the fit are sensitive to the interference between the SM and leptoquark contributions, hence only the real part of the $\delta g_I^{\ell_i}$ is constrained.

4 Results and discussion

Below we study the extent to which the experimental anomalies in $R_{D^{(*)}}$, $R_{K^{(*)}}$ and $(g-2)_\mu$ can be accommodated in light of the constraints presented in Sec. 3.2. We first consider each anomaly separately and then present the combined parameter space.

For all of the random scans in this section our Monte Carlo strategy proceeds as follows. We sample random real values of the free parameters x_{ij} for $i, j \neq 1$ and leptoquark masses in the range $\hat{m}_\phi \in [0.6, 5]$. Values are sampled from the region described in Eq. (3.31)—a necessary condition for the x_{ij} to respect the bound from $B \rightarrow K\nu\nu$, discussed in Sec. 3.2.3—and the perturbativity bound $|x_{ij}| \leq \sqrt{4\pi}$ is imposed at sampling. The values chosen for the right-handed couplings y_{ij} depend on the process studied, although we find that only the y_{2i} and y_{32} are important for our analysis. Two scans are performed, here labelled I and II. Scan I explores the parameter space associated with $R_{K^{(*)}}$ and thus only contains the couplings featuring in Eq. (3.8), while scan II is intended to elucidate the parameter space associated with both $R_{K^{(*)}}$ and $R_{D^{(*)}}$, hence y_{32} is included. An important difference between scans I and II is that the former allows $C_{LR}^\phi \neq 0$, although this comes at the expense of fewer points passing all of the constraints since the couplings y_{22} and y_{23} are heavily constrained by semileptonic charged current processes discussed in Sec. 3.2.1. Explicitly, the parameters and respective ranges over which they are scanned are as follows.

Scan I. $6 \cdot 10^6$ points sampled from the region in Eq. (3.31) subject to

- $\hat{m}_\phi \in [0.6, 5]$,
- $|x_{ij}| \leq \sqrt{4\pi}$ for $i, j \neq 1$,
- $|y_{22}|, |y_{23}| \leq \sqrt{4\pi}$,
- All other couplings are set to zero.

Of the $6 \cdot 10^6$ points, only $\sim 5 \cdot 10^3$ pass all of the constraints.

Scan II. $6 \cdot 10^6$ points sampled from the region in Eq. (3.31) subject to

- $\hat{m}_\phi \in [0.6, 5]$,
- $|x_{ij}| \leq \sqrt{4\pi}$ for $i, j \neq 1$,
- $|y_{23}| \leq 0.05, |y_{32}| \leq \sqrt{4\pi}$,
- All other couplings, including y_{22} , are set to zero.

We will see from the results of scan I that $y_{22} \approx 0$ is preferred for $R_{K^{(*)}}$, hence we take it to vanish in scan II. The range $|y_{23}| \leq 0.05$ is motivated *a posteriori* by the fit to $(g-2)_\mu$ and the avoidance of a number of constraints. These relaxed requirements on the y_{2i} mean that, of the $6 \cdot 10^6$ generated points, $\sim 3.7 \cdot 10^4$ pass all of the constraints.

For each of the points the relevant observables and operators R_D , R_{D^*} , C_{LL}^ϕ and C_{LR}^ϕ are calculated and then the associated coupling constants are filtered through the constraints considered, including $R_K^{\nu\nu} < 4.3$.

Our analysis mainly focuses on answering the following questions: (1) To what extent can the present leptoquark model explain $R_{K^{(*)}}$ while maintaining a SM-like $R_{D^{(*)}}$? (2) To what extent can it explain $R_{D^{(*)}}$ with a SM-like $R_{K^{(*)}}$? (3) How well can all of the anomalies be explained together? (4) Can neutrino masses be explained in the regions relevant for the flavor anomalies? Questions (1)–(3) are addressed below in that order, while (4) is addressed in Sec. 4.2. Throughout this discussion, the relative ease with which this leptoquark model can explain the tension in $(g-2)_\mu$ is exploited to simplify our study. We do not include its calculation in our numerical scans, since the values of x_{23} and y_{23} required—namely, those satisfying Eq. (3.12)—are such that no constraints are encountered.

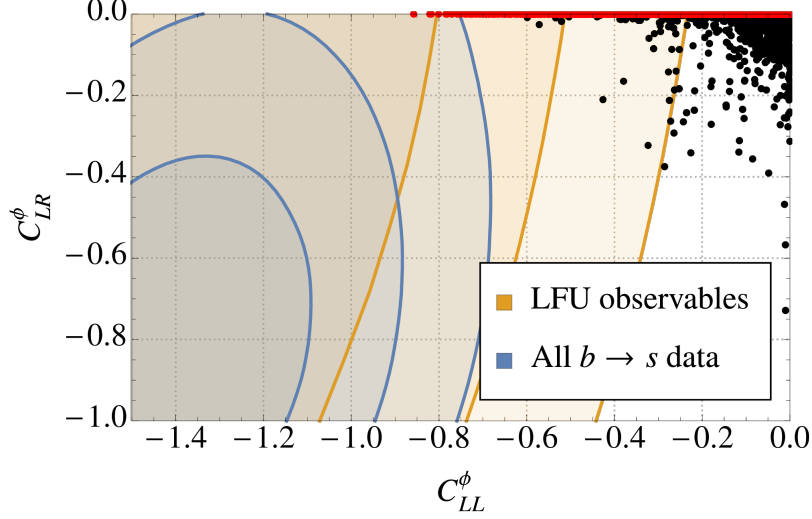
4.1 Flavor anomalies

Explaining $R_{K^{(*)}}$. In order for the leptoquark model to explain the measured tensions in the $b \rightarrow s$ transition the left-handed couplings of ϕ to the second and third generation of quarks are necessary to ensure a non-vanishing C_{LL}^ϕ , a parameter space very heavily constrained by the limits from rare meson decays discussed in Sec. 3.2.3. The necessary condition Eq. (3.31) imposed by the bound on $R_K^{\nu\nu}$ can be combined with Eq. (3.8a) to give [40]

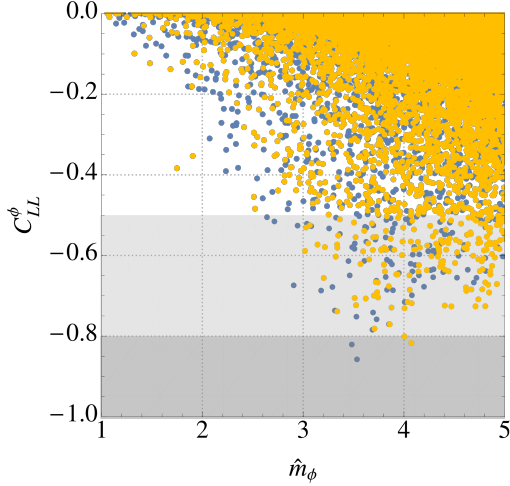
$$\begin{aligned} \sum_{i=1}^2 |z_{2i}|^2 + \left(1 - \frac{0.77}{\hat{m}_\phi^2}\right) |z_{23}|^2 &\approx (|V_{us}|^2 + 1) |z_{22}|^2 + \left(1 - \frac{0.8}{\hat{m}_\phi^2}\right) |z_{23}|^2 \\ &\gtrsim -6C_{LL}^\phi. \end{aligned} \quad (4.1)$$

It follows that $\mathcal{O}(1)$ couplings to the muon are necessary for the model to meet the benchmark $C_{LL}^\phi \approx -1.2$. For small leptoquark masses the model prefers a large $|z_{22}|$ since the top contribution is suppressed through destructive interference between the box diagrams in Fig. 3, however the limit from $D^0 \rightarrow \mu\mu$ [see Eq. (3.39)] prohibits such a scenario. Indeed, the analysis of Ref. [41] indicates that the constraint following from the LFU evident in $R_D^{\mu/e}$ also constitutes a very serious stumbling-block for the model’s explanation of the $b \rightarrow s$ data for $m_\phi \lesssim 1$ TeV. We make progress by performing a random scan in which the leptoquark mass is allowed to vary up to 5 TeV—such large masses have the effect of lifting the suppression on the last term in Eq. (4.1) and permitting larger values for z_{22} according to Eq. (3.39). In addition to the x_{ij} , we turn on the y_{2i} with $i \neq 1$ in order to study the extent to which C_{LR}^ϕ can contribute. These define the parameters of scan I, introduced above, and we present the results of this scan along with those of scan II, for which $C_{LR} = 0$, in Fig. 9 and Fig. 10. We highlight those points for which the $R_{D^{(*)}}$ observables remain SM-like, that is, within twice the theoretical error associated with the SM predictions we cite in Table 1. Consistent with our comments in Section 3.2.1, we find that any phenomenologically viable explanation of the anomalous $b \rightarrow s$ data in this leptoquark model requires $m_\phi \gtrsim 2.5$ TeV. Additionally, constraints from the $\tau \rightarrow \mu$ flavor-changing observables require $|x_{32}| > |x_{33}|$ for large $|x_{32}|$. Although the benchmark value $C_{LL}^\phi \approx -1.2$ is unattainable in light of the constraints we have considered for a perturbative x_{23} , the model can reduce the tension in $R_{K^{(*)}}$ to within 1σ , a significant improvement on the SM. Points in parameter space implying such large, negative values for C_{LL}^ϕ also entail a vanishing C_{LR} , although even in this region agreement with all of the $b \rightarrow s$ data can be slightly better than 3σ .

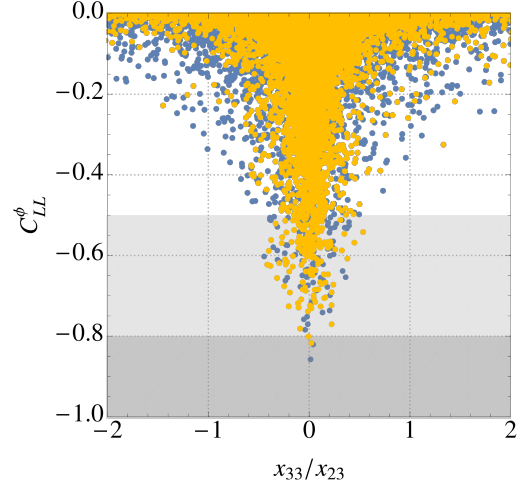
Explaining $R_{D^{(*)}}$. We move on to consider the extent to which the leptoquark can explain the anomalies in the $b \rightarrow c$ transition. The fit presented in Fig. 2 suggests two scenarios for explaining the measured tensions in the $b \rightarrow c\ell\nu$ decays in the region A: (i) new physics only in C_V^{33} , or (ii) new-physics in C_V^{33} along with contributions from C_S^{33} and C_T^{33} . Possibility (i) is consistent with the best-fit value, and this is the region of parameter space considered in the model’s original form. However, we emphasize that the conditions presented in Eq. (3.31) and Eq. (3.50) are sufficient to preclude that effects in C_V^{33} alone could be responsible for the enhancement of the $R_{D^{(*)}}$ ratios. The product $x_{32}^*x_{33}$ is heavily constrained from $R_K^{\nu\nu}$ and $B_s-\bar{B}_s$ mixing, as indicated in Fig. 8. One could consider generating z_{23} , and therefore C_V^{33} , through quark mixing, thus making do only with a non-zero x_{33} and avoiding these constraints. This set-up, however, requires excessively large values of x_{33} to explain $R_{D^{(*)}}$, causing the leptoquark’s contributions to the $Z\tau\bar{\tau}$ coupling to exceed current experimental limits—a result we illustrate in Fig. 11. In addition, we find the effects of lepton-flavor violation to be subdued, since such contributions add incoherently to the W -mediated SM processes, and thus entail couplings large enough to conflict with measurements of $B_s-\bar{B}_s$ mixing and precision electroweak observables. Scenario (ii) involves new physics in C_S^{ij} and C_T^{ij} . The most minimal approach here is to turn on only the bottom–tau-neutrino interaction x_{33} and the right-handed tau–charm coupling y_{32} . A non-zero x_{33} will generate C_V^{33} through quark-mixing. We find the coupling y_{32} to be weakly constrained



(a) The results of scan I (black) and scan II (red) projected onto the C_{LL}^ϕ - C_{LR}^ϕ plane. The colored contours correspond to those in Fig. 4: the orange represent the fit to only LFU observables while the blue take into account all $b \rightarrow s$ observables. The model can alleviate the tensions in LFU observables to just within the 1σ region, a significant improvement on the SM. In this region, $C_{LR}^\phi \approx 0$, implying a suppression of the y_{2i} . Agreement with all of the $b \rightarrow s$ data is not as good.



(b) A scatter plot showing the results of scan II projected onto the C_{LL}^ϕ - \hat{m}_ϕ plane. Yellow points imply SM-like values for R_D and R_{D^*} . The constraints imposed by $D^0 \rightarrow \mu\mu$, $D^+ \rightarrow \pi^+\mu\mu$ and $Z \rightarrow \mu\bar{\mu}$ disfavor light leptoquark masses.



(c) A scatter plot of C_{LL}^ϕ against the ratio x_{33}/x_{23} for parameters subject to scan II. Again, yellow points correspond to SM-like R_D and R_{D^*} . A large, negative value for C_{LL}^ϕ requires $|x_{23}| > |x_{33}|$ to keep LFV $\tau \rightarrow \mu$ observables at bay.

Figure 9: The key results probing the extent to which the model can explain the tensions in $R_{K^{(*)}}$. Significant improvement from the SM is possible for leptoquark masses between 3 and 5 TeV, $|x_{23}| > |x_{33}|$ and suppressed y_{2i} . The grey areas in (b) and (c) are the 1 and 2σ allowed regions for $R_{K^{(*)}}$.

by the precision electroweak measurements discussed earlier: in the limit $|y_{32}| \gg |y_{3(1,3)}|$, the bound

$$|y_{32}| < \frac{3.69\hat{m}_\phi}{\sqrt{1 + 0.39 \ln \hat{m}_\phi}}, \quad (4.2)$$

follows from Eq. (3.50). In addition, small values of the muon-top coupling y_{23} will allow sizeable contributions to $(g-2)_\mu$ in the presence of $x_{23} \neq 0$ because of the top-mass enhancement in the mixed-chirality term of Eq. (3.11). This minimal texture involving only third-generation couplings to left-handed quarks comes with the additional benefit that the leptoquark can evade the constraints from measurements of $R_K^{\nu\nu}$ and $B_s-\bar{B}_s$ mixing. In fact, the only serious constraint is that arising from the modification of the $Z\tau\bar{\tau}$ coupling from a large x_{33} , a situation that can be remedied for $y_{32} \sim \mathcal{O}(1)$, allowing a good fit to the $R_{D^{(*)}}$ data for slightly smaller values of x_{33} . A sizeable y_{32} is thus a necessary requirement for this leptoquark model to explain the experimental anomalies in R_D and R_{D^*} . For example, the parameter choices $m_\phi = 1$ TeV, $x_{33} = 1.3$ and $y_{32} = 0.3$ are sufficient to explain $R_{D^{(*)}}$ to within 1σ , and this choice of couplings passes all the constraints we impose. Note also that the measured tension in $(g-2)_\mu$ can be accommodated at the same time since the couplings involved are unimportant for $b \rightarrow c\tau\nu$. Saturating both x_{33} and y_{32} at the perturbativity bound $\sqrt{4\pi}$, we find that an explanation of $R_{D^{(*)}}$ loses viability at ~ 10 TeV.

In Fig. 12 we present the results of scan II in the $R_D-R_{D^*}$ plane, while Fig. 13 displays the values of the Yukawa couplings from the same scan that lead to interesting R_D values. Limits on the $B \rightarrow K\nu\nu$ rate and measurements of $B_s-\bar{B}_s$ mixing constrain the x_{i2} to be small, while large values for x_{33} and y_{32} are necessary since their product appears in the expressions for C_V^{33} , C_S^{33} and C_T^{33} . As discussed above, these large x_{33} values imply dangerous contributions to $Z \rightarrow \tau\tau$, causing few points to stray into the 1σ region. The model can, however, significantly reduce the tension in the $b \rightarrow c\tau\nu$ measurements in a large region of parameter space. Agreement with the Belle result from Ref. [26] is better than the combined fit, since this model predicts slightly smaller values of R_{D^*} than those suggested by the BaBar and LHCb measurements.

Explaining both $R_{K^{(*)}}$ and $R_{D^{(*)}}$. In order to establish the full power of the model to explain both $R_{D^{(*)}}$ and $R_{K^{(*)}}$, we perform a complete scan over the 7-dimensional parameter space spanned by the leptoquark mass and the couplings x_{ij} for $i, j \neq 1$, y_{23} and y_{32} —the parameters of scan II. Results from this scan have been presented above in the context of explaining one or the other anomaly separately, although in this case the blue points of Figs. 9b, 9c, 10, 12, 13 and red points of Fig. 9 are relevant. In addition to these, we present the results of scan II in $C_{LL}-R_D-R_{D^*}$ space, where color is used as the third axis, in Fig. 13. This plot demonstrates a mild tension between $R_{K^{(*)}}$ and $R_{D^{(*)}}$ in this leptoquark model: points lying within the 1σ region for $R_{K^{(*)}}$ keep R_{D^*} SM-like, while those breaching the 1σ boundary for R_D and R_{D^*} imply $C_{LL}^\phi \approx 0$. This can be attributed to the behavior evident in Fig. 9c: large, negative values of C_{LL}^ϕ require $x_{33} \approx 0$, but x_{33} is essential to this model’s explanation of $R_{D^{(*)}}$, since it features in $C_{V,S,T}^{33}$. At best, we find that the model can explain all of the discrepant measurements to within 2σ , a striking level

of consistency with all constraints and anomalies. In both cases the $(g-2)_\mu$ anomaly can also be accommodated.

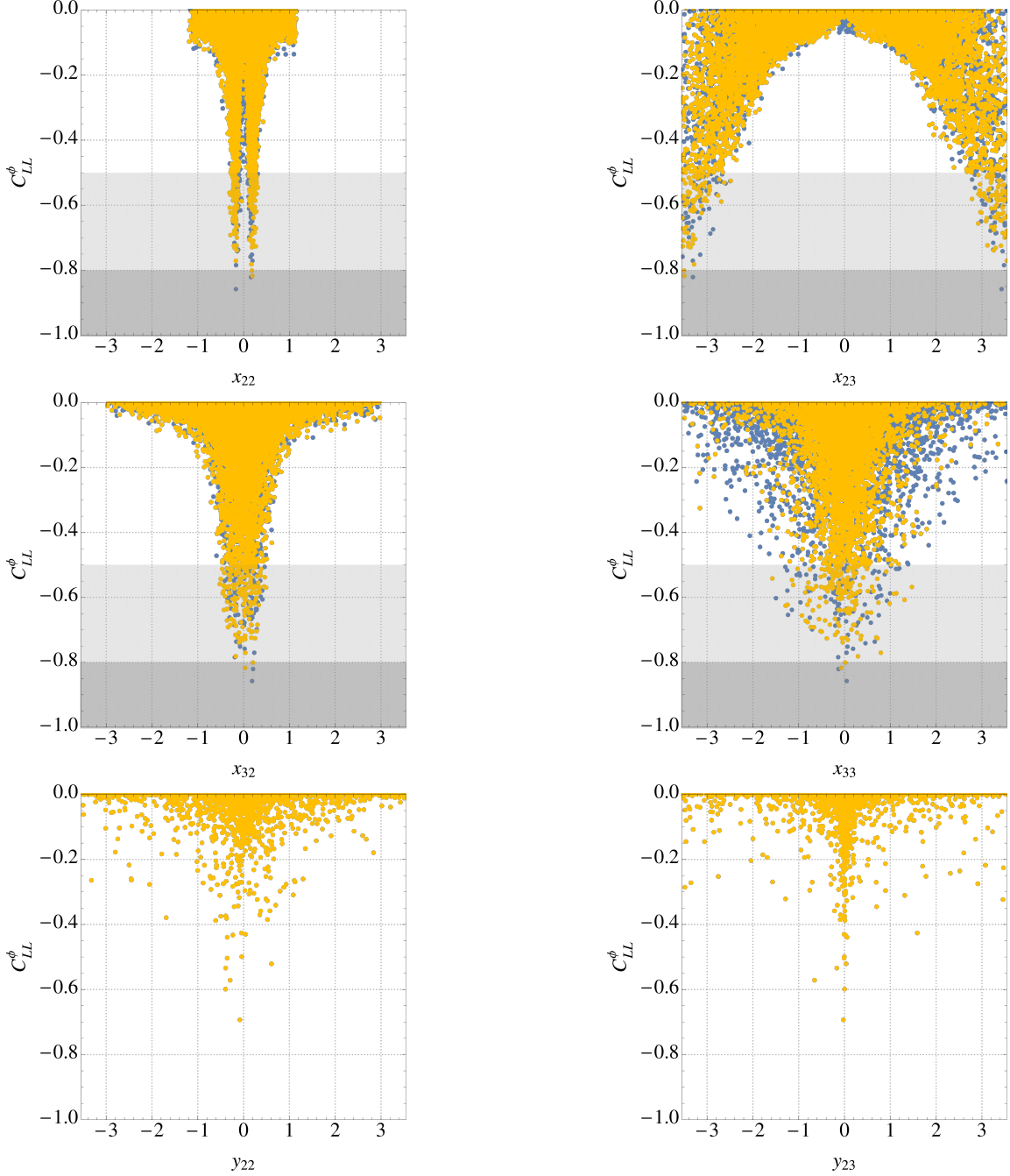


Figure 10: Slices through the parameter space investigated through scans I and II. The value of C_{LL}^ϕ is plotted against each Yukawa coupling scanned over. Plots against the x_{ij} contain points from scan II and hence 1 and 2σ regions for $R_{K^{(*)}}$ can be specified since $C_{LR} = 0$, these are shaded grey, and points implying SM-like $R_{D^{(*)}}$ values are shown in yellow. Plots against the y_{2i} are from scan I, for which all points predict SM-like $R_{D^{(*)}}$ since $y_{32} = 0$. Large values of x_{23} are essential for an adequate explanation of the $b \rightarrow s$ data in this model, while small, but non-zero, values for x_{22} are necessary to allow C_{LL}^ϕ to be negative. The values of x_{23} required to explain the LFU observables to 2σ begin to impinge on the perturbativity constraint $|x_{23}| < \sqrt{4\pi}$.

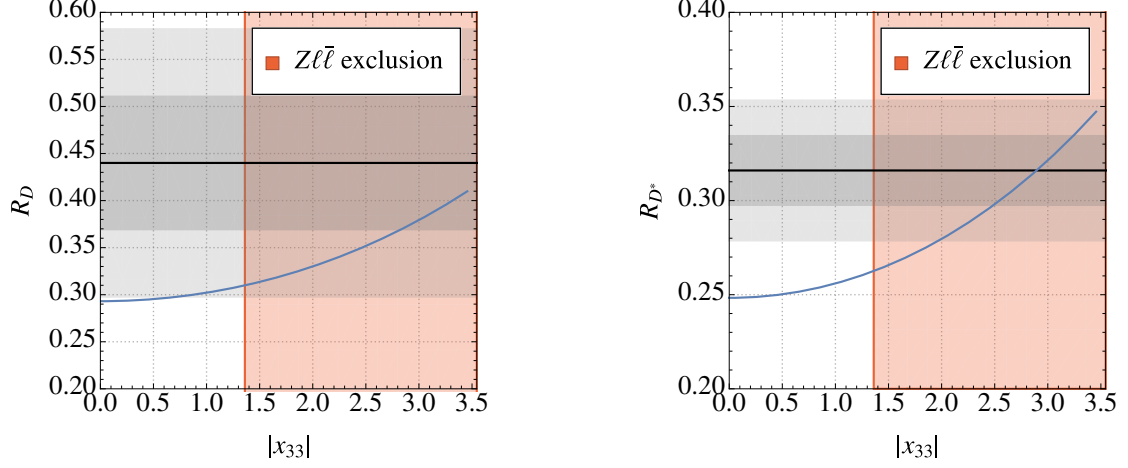


Figure 11: The solid blue lines represents the dependence of R_D (left) and R_{D^*} (right) on $|x_{33}|$ when all other couplings are set to zero and $m_\phi = 1$ TeV. A non-zero x_{33} generates a small z_{32} through the quark mixing of Eq. (2.4), although the $|x_{33}|$ values required to meet the anomalies become large enough to dangerously modify the $Z \rightarrow \tau\tau$ rate. The values of $|x_{33}|$ excluded by measurements of the $Z\tau\tau$ coupling are shaded red. The solid black line represents the central values of the measurements for R_D and R_{D^*} , and the grey areas are the 1 and 2 σ regions.

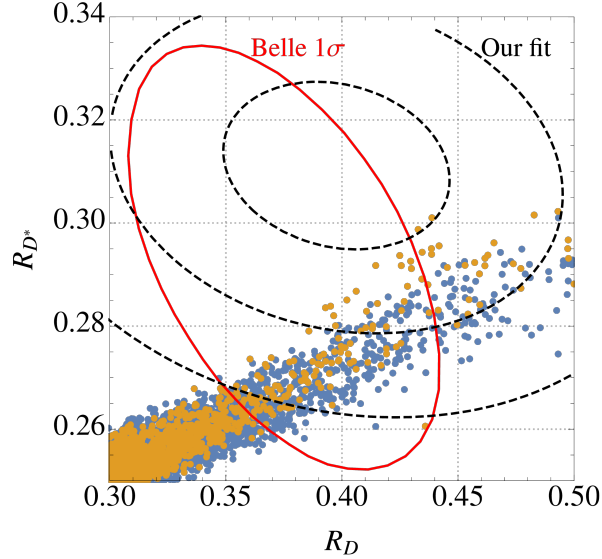


Figure 12: The results of scan II presented as a scatter plot of R_D against R_{D^*} . The orange points keep C_{LL} SM-like, while blue points show a $> 1\%$ deviation in C_{LL} from the SM prediction. The dashed black ellipses represent the 1, 2 and 3 σ contours from our fit with an assumed correlation $\rho = -0.2$, while the solid red curve indicates the 1 σ allowed region implied by the Belle measurement from Ref. [26]. The anomalies in $b \rightarrow c\tau\nu$ can be accommodated in this model, although even small, non-zero values for the x_{i2} cause tension with limits from $B \rightarrow K\nu\nu$ and measurements of $B_s - \bar{B}_s$ mixing, causing few points to stray into the 1 σ region of our fit.

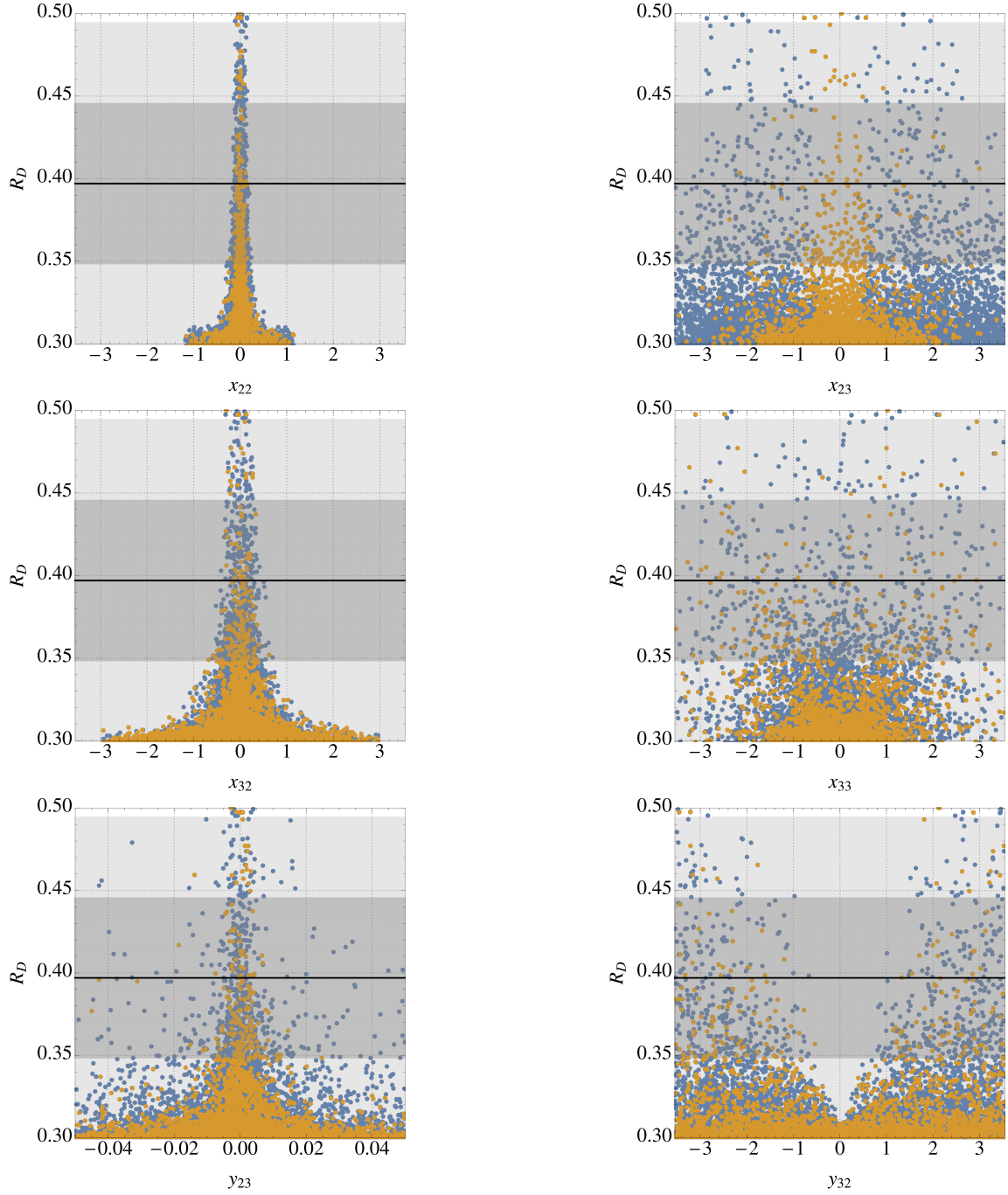


Figure 13: Slices through the parameter space of scan II. The solid black line represents the central value of the R_D measurement, and the grey bands correspond to the 1 and 2σ regions. The orange points keep C_{LL} SM-like, while blue points show $> 1\%$ deviation in C_{LL} from the SM prediction. Large values x_{33} and y_{32} are necessary for an adequate explanation of R_D since these feature in C_S and C_T . Other left-handed couplings must be small to evade constraints from $R_K^{\nu\nu}$ and $B_s-\bar{B}_s$ mixing. The results for R_{D^*} are qualitatively the same.

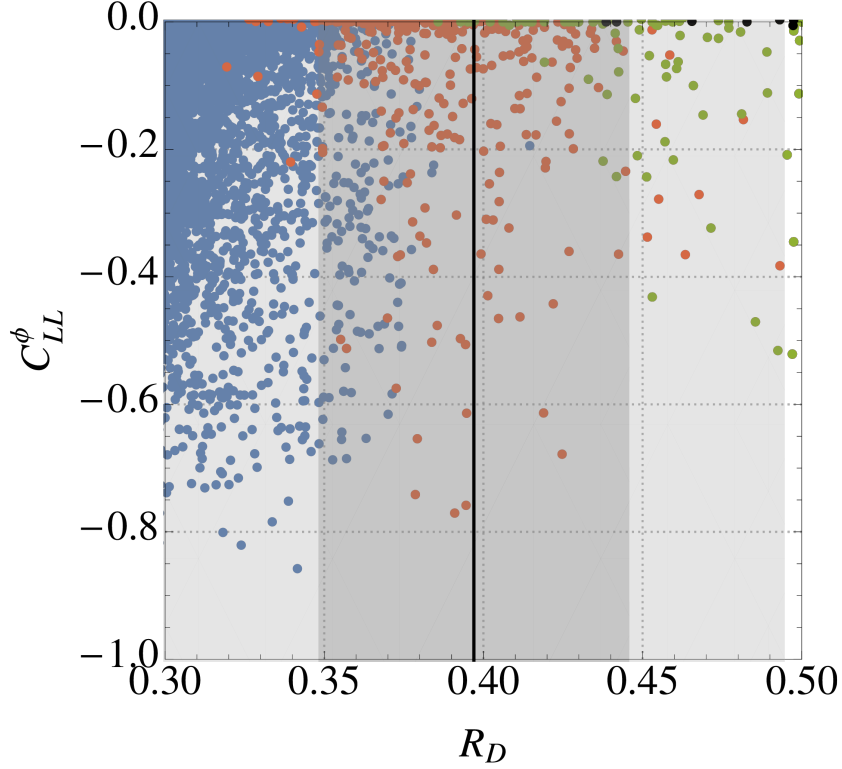


Figure 14: A projection of the random points subject to scan II onto the R_D – C_{LL}^ϕ plane, with colors corresponding to σ -regions of the fit to R_{D^*} : black, green, red and blue points lie in the 1, 2, 3 or $> 3\sigma$ region for R_{D^*} . The solid black line represents the central value of the R_D measurement, and the grey bands correspond to the 1 and 2σ regions. Parameter choices leading to the required large, negative value for C_{LL}^ϕ tend to compromise agreement with measurements of R_{D^*} . A combined explanation of $R_{D^{(*)}}$ and $R_{K^{(*)}}$ is only possible at the 2σ level for both anomalies. This represents a significant improvement on the SM.

4.2 A representative neutrino mass realization

In this section we incorporate the BN leptoquark into the two-loop neutrino mass model developed and studied in detail in Ref. [76]. We summarize the key features of the model below, and point the reader to the original paper for more detail.

Following Ref. [76] we couple the leptoquark ϕ to the color-octet Majorana fermion $f \sim (\mathbf{8}, \mathbf{1}, 0)$ in order to introduce the lepton-number violating terms $m_f f f$ and $w_i \bar{d}_i f \phi$. The dimension-9 $\Delta L = 2$ effective operator $LLQd^c Qd^c$ is generated when the heavy fields f and ϕ are integrated out. The neutrino mass is proportional to the product of down-type quark mass matrices, which is dominated by the bottom quark mass. We do not consider the case where a strong hierarchy in the w_i undermines this dominance, and thus only the coupling to the third generation of quarks (w_3) is important for the neutrino mass generation. For this reason we set $w_{1,2} = 0$ to simplify the calculation of the neutrino mass. In this limit the neutrino mass matrix will have unit rank and an additional generation of the leptoquark ϕ is needed to satisfy current oscillation data. Replacing ϕ with $\phi_a = (\phi_1, \phi_2)$ in Eq. (2.1), small neutrino masses are generated through the two-loop graph shown in Fig. 15 and the neutrino mass is given by

$$M_{ij} \approx 4 \frac{m_f m_b^2}{(2\pi)^8} \sum_{a,b}^2 (x_{i3a} w_{3a}) I_{ab} (x_{j3b} w_{3b}), \quad (4.3)$$

where \mathbf{I} is the matrix of loop integrals in the leptoquark-generation space whose explicit form can be found in Ref. [76]. This expression for the mass matrix can be solved for the x_{i3a} through the Casas–Ibarra procedure [123] to give

$$x_{i3a} = \frac{(2\pi)^4}{2w_{3a} m_b \sqrt{m_f}} U_{ij}^* [\tilde{\mathbf{M}}^{1/2}]_{jk} R_{kb} [\tilde{\mathbf{I}}^{-1/2} \mathbf{S}]_{ba}, \quad (4.4)$$

where tildes denote real and positive diagonal matrices and \mathbf{S} diagonalizes the matrix \mathbf{I} . We use the best-fit values from the NuFIT collaboration for the neutrino mixing angles and mass-squared differences [124, 125]:

$$\begin{aligned} \sin^2 \theta_{12} &= 0.306, & \Delta m_{21}^2 &= 7.50 \cdot 10^{-5} \text{ eV}^2, \\ \sin^2 \theta_{13} &= 0.02166, & \Delta m_{31}^2 &= 2.524 \cdot 10^{-3} \text{ eV}^2 \text{ (NO)}, \\ \sin^2 \theta_{23} &= 0.441 \text{ (NO)}, & \Delta m_{32}^2 &= -2.514 \cdot 10^{-3} \text{ eV}^2 \text{ (IO)}, \\ \sin^2 \theta_{23} &= 0.587 \text{ (IO)}. \end{aligned} \quad (4.5)$$

The mass-squared differences fix the elements of $\tilde{\mathbf{M}}$, since the lightest neutrino in this model is almost massless. In the cases of normal and inverted neutrino mass hierarchy,

$$\mathbf{R}^{\text{NO}} = \begin{pmatrix} 0 & 0 \\ \cos \theta & -\sin \theta \\ \sin \theta & \cos \theta \end{pmatrix}, \quad \mathbf{R}^{\text{IO}} = \begin{pmatrix} \cos \theta & -\sin \theta \\ \sin \theta & \cos \theta \\ 0 & 0 \end{pmatrix}, \quad (4.6)$$

and $\theta \in \mathbb{C}$ parameterizes the leptoquark–fermion Yukawa couplings through Eq. (4.4) in such a way that the correct pattern of neutrino masses and mixings is produced. Here

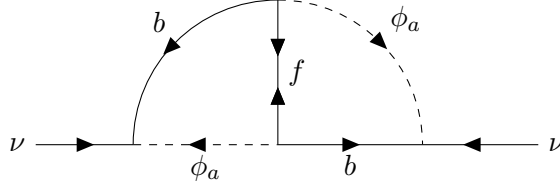


Figure 15: Two loop neutrino mass generation in the model of Ref. [76]. For simplicity we consider the case where the leptoquark ϕ couples significantly only to the third generation of quarks. At least two flavors of ϕ are required to meet the neutrino data.

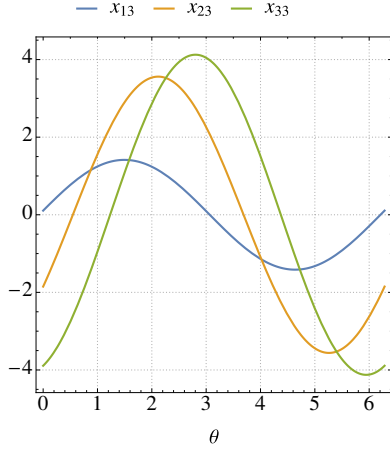
we consider the region of parameter space where $m_{\phi_2}, m_f \gg m_{\phi_1}$ so that ϕ_1 comes to be identified as the BN leptoquark, while ϕ_2 and f are effectively divorced from the flavor anomalies. For this reason we refer to ϕ_1 simply as ϕ and suppress the leptoquark-flavor indices for the remainder of the discussion unless a distinction is necessary. The limit $m_{\phi_1} \ll m_{\phi_2}$ also allows for a simplification in the matrix product $\tilde{\mathbf{I}}^{-1/2} \mathbf{S}$ featuring in Eq. (4.4):

$$\tilde{\mathbf{I}}^{-1/2} \mathbf{S} \approx I_{11}^{-1/2} \begin{pmatrix} -i & i/\epsilon \\ 1 & \epsilon \end{pmatrix}, \quad (4.7)$$

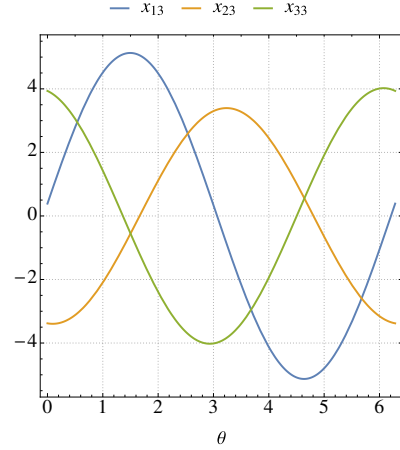
where $\epsilon \equiv I_{12}/I_{11} \ll 1$. This flavor structure implies that its contribution to neutrino mixing is small, and thus the PMNS parameters are principally determined by the Yukawa couplings x_{i3a} . We exploit this relative insensitivity to m_f and m_{ϕ_2} to simplify our analysis in the following.

The decoupling of f and ϕ_2 from the relevant flavor physics makes w_3 an effectively free parameter that acts as a lepton-flavor-blind scaling factor on the couplings of the leptoquark to the third generation of quarks, while θ governs their relative sizes for a given leptoquark flavor. We plot the x_{i3} against real θ values in Fig. 16 for the mass choices $m_f = 25$ TeV, $m_{\phi_2} = 20$ TeV and $m_{\phi_1} = 4$ TeV with fixed $w_3 = 0.003$. Both the normal and inverted hierarchies are considered.

Both Fig. 16 and Eq. (4.4) indicate that, with the inclusion of neutrino mass, the couplings to the electron and electron-neutrino cannot be turned off *ad libitum*. Even a small electron coupling $z_{13} \neq 0$ can generate dangerous contributions to muon–electron conversion in nuclei in the presence of $z_{23} \neq 0$, necessary for the model to alleviate the tensions in the $b \rightarrow s$ transition. We plot the current limit from muon–electron conversion experiments in gold nuclei $\text{Br}(\mu_{79}^{197} \text{Au} \rightarrow e_{79}^{197} \text{Au}) < 7.0 \cdot 10^{-13}$ [98] against θ and w_3 in Fig. 17 for both the normal and inverted hierarchies and a range of masses m_{ϕ_1} . The prospective limit from the COMET experiment: $\text{Br} \sim 10^{-16}$ [126], is also shown. A fit to the neutrino oscillation data while respecting measurements of muon–electron conversion implies a fine-tuning in θ —or, equivalently, z_{31} —to arrange $|z_{31}| \ll |z_{33}|$, pushing the model into a very specific region of parameter space. The required $x_{31} \approx 0$ can be arranged with $\theta \approx 3.08 \pm n\pi$, fixing the ratio $x_{33}/x_{32} = 1.96$ for the normal neutrino mass hierarchy, and $x_{33}/x_{32} = -0.85$ for the inverted hierarchy. Comparison with Fig. 9c, however, indicates that neither of the aforementioned ratios can allow large contributions to $R_{K^{(*)}}$ in the



(a) Normal neutrino mass hierarchy.



(b) Inverted neutrino mass hierarchy.

Figure 16: Plots of the relative sizes of the couplings of the leptoquark ϕ_1 to the bottom quark and the i th neutrino flavor against θ , the Casas–Ibarra parameter, for $m_f = 25$ TeV, $m_{\phi_2} = 20$ TeV, $m_{\phi_1} = 4$ TeV and $w_3 = 0.003$. We only consider the case $\theta \in \mathbb{R}$ here.

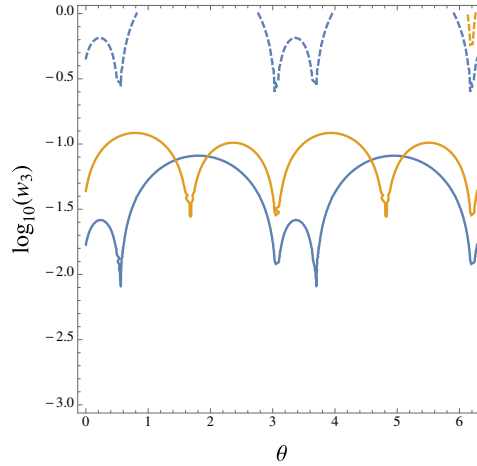


Figure 17: The figure shows the current (solid) and expected [126] (dashed) limits from muon–electron conversion in nuclei in the θ – w_3 plane for normal mass ordering (blue) and inverted ordering (orange). The region below each curve is ruled out. The dips at $\theta \approx 3.08$ and $\theta \approx 6.22$ stretch to negative infinity. Aside from accidental cancellation, the values $\theta \approx 3.08, 6.22$ ensure that the coupling to the electron vanishes. Only real values of θ are considered.

correct direction, although the inverted hierarchy does slightly better than the normal mass ordering. This makes a combined explanation of the $b \rightarrow s$ anomalies and neutrino mass in this model problematic. If, instead, one required that this model explain $R_{D^{(*)}}$, $(g-2)_\mu$ and neutrino mass, the values of x_{33} required are compatible with both the normal and inverted hierarchies, and the model remains agnostic with respect to its preference.

5 Conclusions

We have reconsidered the potential of a scalar leptoquark $\phi \sim (\mathbf{3}, \mathbf{1}, -1/3)$ to explain recent B -physics anomalies—the LFU ratios $R_{K^{(*)}}$ and $R_{D^{(*)}}$, anomalies in branching ratio data and angular observables in the $b \rightarrow s$ transition, as well as the anomalous magnetic moment of the muon.

The leptoquark can reduce the tension in the $R_{D^{(*)}}$ observables to within 1σ of their current experimental values at the price of a sizeable coupling to the right-handed tau and charm quark. The explanation loses viability for masses above about 10 TeV. The leptoquark can also reduce the tensions in the $b \rightarrow s$ data, particularly the LFU observables R_K and R_{K^*} , albeit at some expense to the explanation of $R_{D^{(*)}}$. Explicitly, the region of parameter space in which $R_{D^{(*)}}$ is accommodated to within 1σ implies $R_{K^{(*)}}$ values differing from SM prediction by $< 1\%$, and coupling textures explaining $R_{K^{(*)}}$ to within 1σ keep $R_{D^{(*)}}$ within theoretical uncertainty from SM prediction. At best, we find that the model can accommodate the combined tension from both $R_{K^{(*)}}$ and $R_{D^{(*)}}$ to within 2σ as well as eliminate the tension in $(g-2)_\mu$, a remarkable feat for a single-particle extension of the SM.

A crucial new ingredient for this model’s explanation of $R_{D^{(*)}}$ is the consideration of the area of parameter space in which the coupling y_{32} is large. The combination of right- and left-handed couplings induces scalar and tensor operators, which lift the chirality suppression of the B -meson decays and consequently produce a sizeable new-physics contribution. Moreover the tensor contribution resolves a possible tension induced by the scalar contribution to leptonic charmed B -meson decays, $B_c \rightarrow \tau \nu$. In our numerical scans we found that the right-handed Yukawa coupling y_{32} need take $\mathcal{O}(1)$ values, while the left-handed couplings x_{22} and x_{32} and the right-handed coupling y_{22} are required to be small. Interestingly, this model predicts a value of R_{D^*} slightly smaller than that suggested by current data, consistent with the Belle results.

An explanation of $R_{K^{(*)}}$ requires $\mathcal{O}(1)$ couplings of the leptoquark to the muon, a scenario in conflict with the experimental measurements of the decays of the Z boson and D^0 mesons in the context of this leptoquark model. Moreover, the tension between $R_{K^{(*)}}$ and the lepton universality ratio $R_{D^{(*)}}^{\mu/e}$, pointed out in Ref. [41], is naturally relieved for leptoquark masses $m_\phi \gtrsim 1$ TeV. Consequently, the best fit to $R_{K^{(*)}}$ (requiring large, negative values of C_{LL}^ϕ) is obtained for large leptoquark masses of ~ 5 TeV with a large hierarchy between the left-handed couplings $|x_{32}| \gg |x_{33}|$ to avoid constraints from $\tau \rightarrow \mu$ LFV transitions.

Apart from the anomalies in lepton flavor universality ratios, the leptoquark can easily account for the anomalous magnetic moment of the muon by an appropriate choice of the product of couplings $y_{23}z_{23}$. Moreover, the leptoquark appears naturally in models of neutrino mass [75, 76, 107, 127]. We explicitly demonstrate the possibility to explain $R_{D^{(*)}}$ in the two-loop neutrino mass model proposed in Ref. [76].

At a future 100 TeV proton–proton collider the pair-production cross section of the leptoquark will be substantially enhanced compared to the LHC with about 1 fb for a 5 TeV leptoquark [128] and thus will be able to probe most of the relevant parameter space

for the B -physics anomalies studied here.

Acknowledgments

This work was supported in part by the Australian Research Council. We thank Innes Bigaran, Alexander Ermakov and Phillip Urquijo for discussions on the flavor anomalies. We also thank Damir Bečirević, Christoph Bobeth, Jorge Camalich, Andreas Crivellin, Diptimoy Ghosh, Gudrun Hiller, Soumitra Nandi, Mariano Quiros, Olcyr Sumensari and Javier Virto for helpful correspondence. JG thanks the organisers of the ‘Instant workshop on B -meson anomalies’ held at CERN for their hospitality and the many valuable discussions that took place there. All Feynman diagrams were generated using the TikZ-Feynman package for L^AT_EX [129].

References

- [1] G. Hiller and F. Krüger, *More model-independent analysis of $b \rightarrow s$ processes*, *Phys. Rev. D* **69** (2004) 074020, [[hep-ph/0310219](#)].
- [2] B. Capdevila, A. Crivellin, S. Descotes-Genon, J. Matias and J. Virto, *Patterns of New Physics in $b \rightarrow s\ell^+\ell^-$ transitions in the light of recent data*, [1704.05340](#).
- [3] B. Capdevila, S. Descotes-Genon, J. Matias and J. Virto, *Assessing lepton-flavour non-universality from $B \rightarrow K^*\ell\ell$ angular analyses*, *JHEP* **10** (2016) 075, [[1605.03156](#)].
- [4] LHCb collaboration, R. Aaij et al., *Test of lepton universality using $B^+ \rightarrow K^+\ell^+\ell^-$ decays*, *Phys. Rev. Lett.* **113** (2014) 151601, [[1406.6482](#)].
- [5] C. Bobeth, G. Hiller and G. Piranishvili, *Angular distributions of $\bar{B} \rightarrow \bar{K}\ell^+\ell^-$ decays*, *JHEP* **12** (2007) 040, [[0709.4174](#)].
- [6] LHCb collaboration, S. Bifani, *Search for new physics with $b \rightarrow s\ell^+\ell^-$ decays at lhcb*, CERN Seminar 18 April, 2017.
- [7] M. Bordone, G. Isidori and A. Pattori, *On the Standard Model predictions for R_K and R_{K^*}* , *Eur. Phys. J. C* **76** (2016) 440, [[1605.07633](#)].
- [8] S. Descotes-Genon, J. Matias and J. Virto, *Understanding the $B \rightarrow K^*\mu^+\mu^-$ Anomaly*, *Phys. Rev. D* **88** (2013) 074002, [[1307.5683](#)].
- [9] S. Descotes-Genon, L. Hofer, J. Matias and J. Virto, *Global analysis of $b \rightarrow s\ell\ell$ anomalies*, *JHEP* **06** (2016) 092, [[1510.04239](#)].
- [10] R. Alonso, B. Grinstein and J. Martin Camalich, $SU(2) \times U(1)$, *Phys. Rev. Lett.* **113** (Dec, 2014) 241802.
- [11] G. Hiller and M. Schmaltz, *R_K and future $b \rightarrow s\ell\ell$ physics beyond the standard model opportunities*, *Phys. Rev. D* **90** (2014) 054014, [[1408.1627](#)].
- [12] D. Ghosh, M. Nardecchia and S. A. Renner, *Hint of Lepton Flavour Non-Universality in B Meson Decays*, *JHEP* **12** (2014) 131, [[1408.4097](#)].
- [13] T. Hurth, F. Mahmoudi and S. Neshatpour, *Global fits to $b \rightarrow s\ell\ell$ data and signs for lepton non-universality*, *JHEP* **12** (2014) 053, [[1410.4545](#)].

- [14] W. Altmannshofer and D. M. Straub, *New physics in $b \rightarrow s$ transitions after LHC run 1*, *Eur. Phys. J. C* **75** (2015) 382, [[1411.3161](#)].
- [15] S. L. Glashow, D. Guadagnoli and K. Lane, *Lepton Flavor Violation in B Decays?*, *Phys. Rev. Lett.* **114** (2015) 091801, [[1411.0565](#)].
- [16] W. Altmannshofer, P. Stangl and D. M. Straub, *Interpreting Hints for Lepton Flavor Universality Violation*, [1704.05435](#).
- [17] M. Ciuchini, A. M. Coutinho, M. Fedele, E. Franco, A. Paul, L. Silvestrini et al., *On Flavourful Easter eggs for New Physics hunger and Lepton Flavour Universality violation*, [1704.05447](#).
- [18] L.-S. Geng, B. Grinstein, S. Jäger, J. Martin Camalich, X.-L. Ren and R.-X. Shi, *Towards the discovery of new physics with lepton-universality ratios of $b \rightarrow s\ell\ell$ decays*, [1704.05446](#).
- [19] G. D’Amico, M. Nardecchia, P. Panci, F. Sannino, A. Strumia, R. Torre et al., *Flavour anomalies after the R_{K^*} measurement*, [1704.05438](#).
- [20] A. Bharucha, D. M. Straub and R. Zwicky, *$B \rightarrow V\ell^+\ell^-$ in the Standard Model from light-cone sum rules*, *JHEP* **08** (2016) 098, [[1503.05534](#)].
- [21] J. Lyon and R. Zwicky, *Resonances gone topsy turvy - the charm of QCD or new physics in $b \rightarrow s\ell^+\ell^-$?*, [1406.0566](#).
- [22] S. Descotes-Genon, L. Hofer, J. Matias and J. Virto, *On the impact of power corrections in the prediction of $B \rightarrow K^*\mu^+\mu^-$ observables*, *JHEP* **12** (2014) 125, [[1407.8526](#)].
- [23] S. Jäger and J. Martin Camalich, *Reassessing the discovery potential of the $B \rightarrow K^*\ell^+\ell^-$ decays in the large-recoil region: SM challenges and BSM opportunities*, *Phys. Rev. D* **93** (2016) 014028, [[1412.3183](#)].
- [24] BABAR collaboration, J. P. Lees et al., *Evidence for an excess of $\bar{B} \rightarrow D^{(*)}\tau^-\bar{\nu}_\tau$ decays*, *Phys. Rev. Lett.* **109** (2012) 101802, [[1205.5442](#)].
- [25] BABAR collaboration, J. P. Lees et al., *Measurement of an Excess of $\bar{B} \rightarrow D^{(*)}\tau^-\bar{\nu}_\tau$ Decays and Implications for Charged Higgs Bosons*, *Phys. Rev. D* **88** (2013) 072012, [[1303.0571](#)].
- [26] BELLE collaboration, M. Huschle et al., *Measurement of the branching ratio of $\bar{B} \rightarrow D^{(*)}\tau^-\bar{\nu}_\tau$ relative to $\bar{B} \rightarrow D^{(*)}\ell^-\bar{\nu}_\ell$ decays with hadronic tagging at Belle*, *Phys. Rev. D* **92** (2015) 072014, [[1507.03233](#)].
- [27] BELLE collaboration, Y. Sato et al., *Measurement of the branching ratio of $\bar{B}^0 \rightarrow D^{*+}\tau^-\bar{\nu}_\tau$ relative to $\bar{B}^0 \rightarrow D^{*+}\ell^-\bar{\nu}_\ell$ decays with a semileptonic tagging method*, *Phys. Rev. D* **94** (2016) 072007, [[1607.07923](#)].
- [28] BELLE collaboration, S. Hirose et al., *Measurement of the τ lepton polarization and $R(D^*)$ in the decay $\bar{B} \rightarrow D^*\tau^-\bar{\nu}_\tau$* , [1612.00529](#).
- [29] LHCb collaboration, R. Aaij et al., *Measurement of the ratio of branching fractions $\mathcal{B}(\bar{B}^0 \rightarrow D^{*+}\tau^-\bar{\nu}_\tau)/\mathcal{B}(\bar{B}^0 \rightarrow D^{*+}\mu^-\bar{\nu}_\mu)$* , *Phys. Rev. Lett.* **115** (2015) 111803, [[1506.08614](#)].
- [30] Y. Sakaki, M. Tanaka, A. Tayduganov and R. Watanabe, *Testing leptoquark models in $\bar{B} \rightarrow D^{(*)}\tau\bar{\nu}$* , *Phys. Rev. D* **88** (2013) 094012, [[1309.0301](#)].
- [31] D. Bardhan, P. Byakti and D. Ghosh, *A closer look at the R_D and R_{D^*} anomalies*, *JHEP* **01** (2017) 125, [[1610.03038](#)].
- [32] M. Freytsis, Z. Ligeti and J. T. Ruderman, *Flavor models for $\bar{B} \rightarrow D^{(*)}\tau\bar{\nu}$* , *Phys. Rev. D* **92** (2015) 054018, [[1506.08896](#)].

- [33] D. Choudhury, A. Kundu, S. Nandi and S. K. Patra, *Unified resolution of the $R(D)$ and $R(D^*)$ anomalies and the lepton flavor violating decay $h \rightarrow \mu\tau$* , *Phys. Rev.* **D95** (2017) 035021, [[1612.03517](#)].
- [34] S. Bhattacharya, S. Nandi and S. K. Patra, *Looking for possible new physics in $B \rightarrow D^{(*)}\tau\nu_\tau$ in light of recent data*, *Phys. Rev.* **D95** (2017) 075012, [[1611.04605](#)].
- [35] S. Bhattacharya, S. Nandi and S. K. Patra, *Optimal-observable analysis of possible new physics in $B \rightarrow D^{(*)}\tau\nu_\tau$* , *Phys. Rev.* **D93** (2016) 034011, [[1509.07259](#)].
- [36] HEAVY FLAVOR AVERAGING GROUP collaboration, Y. Amhis et al., *Averages of B -Hadron, C -Hadron, and tau-lepton properties as of early 2012*, [1207.1158](#).
- [37] MILC collaboration, J. A. Bailey et al., *$B \rightarrow D\ell\nu$ form factors at nonzero recoil and $|V_{cb}|$ from 2+1-flavor lattice QCD*, *Phys. Rev.* **D92** (2015) 034506, [[1503.07237](#)].
- [38] M. Tanaka and R. Watanabe, *New physics in the weak interaction of $\bar{B} \rightarrow D^{(*)}\tau\bar{\nu}$* , *Phys. Rev.* **D87** (2013) 034028, [[1212.1878](#)].
- [39] R. Alonso, B. Grinstein and J. Martin Camalich, *Lepton universality violation and lepton flavor conservation in B -meson decays*, *JHEP* **10** (2015) 184, [[1505.05164](#)].
- [40] M. Bauer and M. Neubert, *Minimal Leptoquark Explanation for the $R_{D^{(*)}}$, R_K , and $(g-2)_\mu$ Anomalies*, *Phys. Rev. Lett.* **116** (2016) 141802, [[1511.01900](#)].
- [41] D. Bečirević, N. Košnik, O. Sumensari and R. Zukanovich Funchal, *Palatable Leptoquark Scenarios for Lepton Flavor Violation in Exclusive $b \rightarrow s\ell_1\ell_2$ modes*, *JHEP* **11** (2016) 035, [[1608.07583](#)].
- [42] D. Bečirević, S. Fajfer, N. Košnik and O. Sumensari, *Leptoquark model to explain the B -physics anomalies, R_K and R_D* , *Phys. Rev.* **D94** (2016) 115021, [[1608.08501](#)].
- [43] S. M. Boucenna, A. Celis, J. Fuentes-Martin, A. Vicente and J. Virto, *Non-abelian gauge extensions for B -decay anomalies*, *Phys. Lett.* **B760** (2016) 214–219, [[1604.03088](#)].
- [44] S. M. Boucenna, A. Celis, J. Fuentes-Martin, A. Vicente and J. Virto, *Phenomenology of an $SU(2) \times SU(2) \times U(1)$ model with lepton-flavour non-universality*, *JHEP* **12** (2016) 059, [[1608.01349](#)].
- [45] L. Calibbi, A. Crivellin and T. Ota, *Effective Field Theory Approach to $b \rightarrow s\ell\ell^{(\prime)}$, $B \rightarrow K^{(*)}\nu\bar{\nu}$ and $B \rightarrow D^{(*)}\tau\nu$ with Third Generation Couplings*, *Phys. Rev. Lett.* **115** (2015) 181801, [[1506.02661](#)].
- [46] A. Crivellin, D. Müller and T. Ota, *Simultaneous Explanation of $R(D^{(*)})$ and $b \rightarrow s\mu^+\mu^-$: The Last Scalar Leptoquarks Standing*, [1703.09226](#).
- [47] F. F. Deppisch, S. Kulkarni, H. Päs and E. Schumacher, *Leptoquark patterns unifying neutrino masses, flavor anomalies, and the diphoton excess*, *Phys. Rev.* **D94** (2016) 013003, [[1603.07672](#)].
- [48] N. G. Deshpande and X.-G. He, *Consequences of R -parity violating interactions for anomalies in $\bar{B} \rightarrow D^{(*)}\tau\bar{\nu}$ and $b \rightarrow s\mu^+\mu^-$* , *Eur. Phys. J.* **C77** (2017) 134, [[1608.04817](#)].
- [49] S. Fajfer and N. Košnik, *Vector leptoquark resolution of R_K and $R_{D^{(*)}}$ puzzles*, *Phys. Lett.* **B755** (2016) 270–274, [[1511.06024](#)].
- [50] F. Feruglio, P. Paradisi and A. Pattori, *Revisiting Lepton Flavor Universality in B Decays*, *Phys. Rev. Lett.* **118** (2017) 011801, [[1606.00524](#)].

- [51] F. Feruglio, P. Paradisi and A. Pattori, *On the Importance of Electroweak Corrections for B Anomalies*, [1705.00929](#).
- [52] E. Megias, M. Quiros and L. Salas, *Lepton-flavor universality violation in $R_{D^{(*)}}$ and R_K from warped space*, [1703.06019](#).
- [53] O. Popov and G. A. White, *One Leptoquark to unify them? Neutrino masses and unification in the light of $(g-2)_\mu$, $R_{D^{(*)}}$ and R_K anomalies*, [1611.04566](#).
- [54] D. Bečirević, S. Fajfer and N. Košnik, *Lepton flavor nonuniversality in $b \rightarrow s\ell^+\ell^-$ processes*, *Phys. Rev.* **D92** (2015) 014016, [[1503.09024](#)].
- [55] D. Bečirević and O. Sumensari, *A leptoquark model to accommodate $R_K^{\text{exp}} < R_K^{\text{SM}}$ and $R_{K^*}^{\text{exp}} < R_{K^*}^{\text{SM}}$* , [1704.05835](#).
- [56] A. J. Buras and J. Girrbach, *Left-handed Z' and Z FCNC quark couplings facing new $b \rightarrow s\mu^+\mu^-$ data*, *JHEP* **12** (2013) 009, [[1309.2466](#)].
- [57] R. Gauld, F. Goertz and U. Haisch, *On minimal Z' explanations of the $B \rightarrow K^*\mu^+\mu^-$ anomaly*, *Phys. Rev.* **D89** (2014) 015005, [[1308.1959](#)].
- [58] B. Gripaios, M. Nardecchia and S. A. Renner, *Composite leptoquarks and anomalies in B -meson decays*, *JHEP* **05** (2015) 006, [[1412.1791](#)].
- [59] G. Hiller and M. Schmaltz, *Diagnosing lepton-nonuniversality in $b \rightarrow s\ell\ell$* , *JHEP* **02** (2015) 055, [[1411.4773](#)].
- [60] F. Mahmoudi, S. Neshatpour and J. Virto, *$B \rightarrow K^*\mu^+\mu^-$ optimised observables in the MSSM*, *Eur. Phys. J.* **C74** (2014) 2927, [[1401.2145](#)].
- [61] E. Megias, G. Panico, O. Pujolas and M. Quiros, *A Natural origin for the LHCb anomalies*, *JHEP* **09** (2016) 118, [[1608.02362](#)].
- [62] H. Päs and E. Schumacher, *Common origin of R_K and neutrino masses*, *Phys. Rev.* **D92** (2015) 114025, [[1510.08757](#)].
- [63] S. Sahoo and R. Mohanta, *Leptoquark effects on $b \rightarrow s\nu\bar{\nu}$ and $B \rightarrow K\ell^+\ell^-$ decay processes*, *New J. Phys.* **18** (2016) 013032, [[1509.06248](#)].
- [64] S. Sahoo and R. Mohanta, *Study of the rare semileptonic decays $B_d^0 \rightarrow K^*\ell^+\ell^-$ in scalar leptoquark model*, *Phys. Rev.* **D93** (2016) 034018, [[1507.02070](#)].
- [65] D. Aristizabal Sierra, F. Staub and A. Vicente, *Shedding light on the $b \rightarrow s$ anomalies with a dark sector*, *Phys. Rev.* **D92** (2015) 015001, [[1503.06077](#)].
- [66] I. de Medeiros Varzielas and G. Hiller, *Clues for flavor from rare lepton and quark decays*, *JHEP* **06** (2015) 072, [[1503.01084](#)].
- [67] S. de Boer and G. Hiller, *Flavor and new physics opportunities with rare charm decays into leptons*, *Phys. Rev.* **D93** (2016) 074001, [[1510.00311](#)].
- [68] K. S. Babu and C. N. Leung, *Classification of effective neutrino mass operators*, *Nucl. Phys.* **B619** (2001) 667–689, [[hep-ph/0106054](#)].
- [69] A. de Gouvea and J. Jenkins, *A Survey of Lepton Number Violation Via Effective Operators*, *Phys. Rev.* **D77** (2008) 013008, [[0708.1344](#)].
- [70] P. W. Angel, N. L. Rodd and R. R. Volkas, *Origin of neutrino masses at the LHC: $\Delta L = 2$ effective operators and their ultraviolet completions*, *Phys. Rev.* **D87** (2013) 073007, [[1212.6111](#)].

- [71] K. Cheung, T. Nomura and H. Okada, *Testable radiative neutrino mass model without additional symmetries and explanation for the $b \rightarrow s\ell^+\ell^-$ anomaly*, *Phys. Rev.* **D94** (2016) 115024, [[1610.02322](#)].
- [72] K. Cheung, T. Nomura and H. Okada, *A Three-loop Neutrino Model with Leptoquark Triplet Scalars*, *Phys. Lett.* **B768** (2017) 359–364, [[1701.01080](#)].
- [73] K. Cheung, T. Nomura and H. Okada, *Three-loop neutrino mass model with a colored triplet scalar*, *Phys. Rev.* **D95** (2017) 015026, [[1610.04986](#)].
- [74] K. S. Babu and J. Julio, *Two-Loop Neutrino Mass Generation through Leptoquarks*, *Nucl. Phys.* **B841** (2010) 130–156, [[1006.1092](#)].
- [75] D. Aristizabal Sierra, M. Hirsch and S. G. Kovalenko, *Leptoquarks: Neutrino masses and accelerator phenomenology*, *Phys. Rev.* **D77** (2008) 055011, [[0710.5699](#)].
- [76] P. W. Angel, Y. Cai, N. L. Rodd, M. A. Schmidt and R. R. Volkas, *Testable two-loop radiative neutrino mass model based on an $LLQd^cQd^c$ effective operator*, *JHEP* **10** (2013) 118, [[1308.0463](#)].
- [77] I. Doršner, S. Fajfer, A. Greljo, J. F. Kamenik and N. Košnik, *Physics of leptoquarks in precision experiments and at particle colliders*, *Phys. Rept.* **641** (2016) 1–68, [[1603.04993](#)].
- [78] CMS collaboration, V. Khachatryan et al., *Search for pair production of first and second generation leptoquarks in proton-proton collisions at $\sqrt{s} = 8$ TeV*, *Phys. Rev.* **D93** (2016) 032004, [[1509.03744](#)].
- [79] ATLAS collaboration, G. Aad et al., *Searches for scalar leptoquarks in pp collisions at $\sqrt{s} = 8$ TeV with the ATLAS detector*, *Eur. Phys. J.* **C76** (2016) 5, [[1508.04735](#)].
- [80] B. Dumont, K. Nishiwaki and R. Watanabe, *LHC constraints and prospects for S_1 scalar leptoquark explaining the $\bar{B} \rightarrow D^{(*)}\tau\bar{\nu}$ anomaly*, *Phys. Rev.* **D94** (2016) 034001, [[1603.05248](#)].
- [81] BABAR collaboration, B. Aubert et al., *Determination of the form-factors for the decay $B^0 \rightarrow D^{*-}\ell^+\nu_\ell$ and of the CKM matrix element $|V_{cb}|$* , *Phys. Rev.* **D77** (2008) 032002, [[0705.4008](#)].
- [82] BABAR collaboration, B. Aubert et al., *Measurements of the Semileptonic Decays $\bar{B} \rightarrow D\ell\bar{\nu}$ and $\bar{B} \rightarrow D^*\ell\bar{\nu}$ Using a Global Fit to $D \rightarrow X\ell\bar{\nu}$ Final States*, *Phys. Rev.* **D79** (2009) 012002, [[0809.0828](#)].
- [83] BELLE collaboration, K. Abe et al., *Measurement of $BR(\bar{B}_0 \rightarrow D^+\ell^-\bar{\nu})$ and determination of $|V_{cb}|$* , *Phys. Lett.* **B526** (2002) 258–268, [[hep-ex/0111082](#)].
- [84] BELLE collaboration, W. Dungen et al., *Measurement of the form factors of the decay $B_0 \rightarrow D^*-\ell^+\nu$ and determination of the CKM matrix element $|V_{cb}|$* , *Phys. Rev.* **D82** (2010) 112007, [[1010.5620](#)].
- [85] I. Doršner, S. Fajfer, N. Košnik and I. Nišandžić, *Minimally flavored colored scalar in $\bar{B} \rightarrow D^{(*)}\tau\bar{\nu}$ and the mass matrices constraints*, *JHEP* **11** (2013) 084, [[1306.6493](#)].
- [86] K. G. Chetyrkin, J. H. Kuhn and M. Steinhauser, *RunDec: A Mathematica package for running and decoupling of the strong coupling and quark masses*, *Comput. Phys. Commun.* **133** (2000) 43–65, [[hep-ph/0004189](#)].
- [87] M. Misiak, *The $b \rightarrow se^+e^-$ and $b \rightarrow s\gamma$ decays with next-to-leading logarithmic QCD corrections*, *Nucl. Phys.* **B393** (1993) 23–45.

- [88] BABAR collaboration, J. P. Lees et al., *Measurement of the $B \rightarrow X_s \ell^+ \ell^-$ branching fraction and search for direct CP violation from a sum of exclusive final states*, *Phys. Rev. Lett.* **112** (2014) 211802, [[1312.5364](#)].
- [89] A. Djouadi, T. Kohler, M. Spira and J. Tutas, *(e b), (e t) type leptoquarks at e p collider*, *Z. Phys.* **C46** (1990) 679–686.
- [90] D. Chakraverty, D. Choudhury and A. Datta, *A Nonsupersymmetric resolution of the anomalous muon magnetic moment*, *Phys. Lett.* **B506** (2001) 103–108, [[hep-ph/0102180](#)].
- [91] K.-m. Cheung, *Muon anomalous magnetic moment and leptoquark solutions*, *Phys. Rev.* **D64** (2001) 033001, [[hep-ph/0102238](#)].
- [92] M. Davier, A. Hoecker, B. Malaescu and Z. Zhang, *Reevaluation of the Hadronic Contributions to the Muon $g - 2$ and to $\alpha(M_Z)$* , *Eur. Phys. J.* **C71** (2011) 1515, [[1010.4180](#)].
- [93] S. Aoki et al., *Review of lattice results concerning low-energy particle physics*, *Eur. Phys. J.* **C77** (2017) 112, [[1607.00299](#)].
- [94] R. Alonso, B. Grinstein and J. Martin Camalich, *The lifetime of the B_c^- meson and the anomalies in $B \rightarrow D^{(*)} \tau \nu$* , *Phys. Rev. Lett.* **118** (2017) 081802, [[1611.06676](#)].
- [95] BELLE collaboration, A. Zupanc et al., *Measurements of branching fractions of leptonic and hadronic D_s^+ meson decays and extraction of the D_s^+ meson decay constant*, *JHEP* **09** (2013) 139, [[1307.6240](#)].
- [96] BELLE collaboration, R. Glattauer et al., *Measurement of the decay $B \rightarrow D \ell \nu_\ell$ in fully reconstructed events and determination of the Cabibbo-Kobayashi-Maskawa matrix element $|V_{cb}|$* , *Phys. Rev.* **D93** (2016) 032006, [[1510.03657](#)].
- [97] BELLE collaboration, A. Abdesselam et al., *Precise determination of the CKM matrix element $|V_{cb}|$ with $\bar{B}^0 \rightarrow D^{*+} \ell^- \bar{\nu}_\ell$ decays with hadronic tagging at Belle*, *1702.01521*.
- [98] PARTICLE DATA GROUP collaboration, C. Patrignani et al., *Review of Particle Physics*, *Chin. Phys.* **C40** (2016) 100001.
- [99] V. Cirigliano and I. Rosell, *$\pi/K \rightarrow e \bar{\nu}_e$ branching ratios to $O(e^2 p^4)$ in Chiral Perturbation Theory*, *JHEP* **10** (2007) 005, [[0707.4464](#)].
- [100] M. Finkemeier, *Radiative corrections to π_{l2} and K_{l2} decays*, [hep-ph/9501286](#).
- [101] W. Buchmuller and D. Wyler, *Constraints on $SU(5)$ Type Leptoquarks*, *Phys. Lett.* **B177** (1986) 377–382.
- [102] S. Davidson, D. C. Bailey and B. A. Campbell, *Model independent constraints on leptoquarks from rare processes*, *Z. Phys.* **C61** (1994) 613–644, [[hep-ph/9309310](#)].
- [103] X.-Q. Li, Y.-D. Yang and X. Zhang, *Revisiting the one leptoquark solution to the $R(D^{(*)})$ anomalies and its phenomenological implications*, *JHEP* **08** (2016) 054, [[1605.09308](#)].
- [104] BABAR collaboration, B. Aubert et al., *Searches for Lepton Flavor Violation in the Decays $\tau^+ \rightarrow e^+ \gamma$ and $\tau^+ \rightarrow \mu^+ \gamma$* , *Phys. Rev. Lett.* **104** (2010) 021802, [[0908.2381](#)].
- [105] BELLE collaboration, Y. Miyazaki et al., *Search for Lepton-Flavor-Violating tau Decays into a Lepton and a Vector Meson*, *Phys. Lett.* **B699** (2011) 251–257, [[1101.0755](#)].
- [106] SINDRUM II collaboration, W. H. Bertl et al., *A Search for muon to electron conversion in muonic gold*, *Eur. Phys. J.* **C47** (2006) 337–346.

- [107] Y. Cai, J. D. Clarke, M. A. Schmidt and R. R. Volkas, *Testing Radiative Neutrino Mass Models at the LHC*, *JHEP* **02** (2015) 161, [[1410.0689](#)].
- [108] W. Altmannshofer, A. J. Buras, D. M. Straub and M. Wick, *New strategies for New Physics search in $B \rightarrow K^* \nu \bar{\nu}$, $B \rightarrow K \nu \bar{\nu}$ and $B \rightarrow X_s \nu \bar{\nu}$ decays*, *JHEP* **04** (2009) 022, [[0902.0160](#)].
- [109] A. J. Buras, F. Schwab and S. Uhlig, *Waiting for precise measurements of $K^+ \rightarrow \pi^+ \nu \bar{\nu}$ and $K_L \rightarrow \pi^0 \nu \bar{\nu}$* , *Rev. Mod. Phys.* **80** (2008) 965–1007, [[hep-ph/0405132](#)].
- [110] G. Buchalla and A. J. Buras, *The rare decays $K \rightarrow \pi \nu \bar{\nu}$, $B \rightarrow X \nu \bar{\nu}$ and $B \rightarrow \ell^+ \ell^-$: An Update*, *Nucl. Phys.* **B548** (1999) 309–327, [[hep-ph/9901288](#)].
- [111] M. Misiak and J. Urban, *QCD corrections to FCNC decays mediated by Z penguins and W boxes*, *Phys. Lett.* **B451** (1999) 161–169, [[hep-ph/9901278](#)].
- [112] A. J. Buras, J. Girrbach-Noe, C. Niehoff and D. M. Straub, *$B \rightarrow K^{(*)} \nu \bar{\nu}$ decays in the Standard Model and beyond*, *JHEP* **02** (2015) 184, [[1409.4557](#)].
- [113] G. Kumar, *Constraints on a scalar leptoquark from the kaon sector*, *Phys. Rev.* **D94** (2016) 014022, [[1603.00346](#)].
- [114] BNL-E949 collaboration, A. V. Artamonov et al., *Study of the decay $K^+ \rightarrow \pi^+ \nu \bar{\nu}$ in the momentum region $140 < P_\pi < 199$ MeV/c*, *Phys. Rev.* **D79** (2009) 092004, [[0903.0030](#)].
- [115] LHCb collaboration, R. Aaij et al., *Search for the rare decay $D^0 \rightarrow \mu^+ \mu^-$* , *Phys. Lett.* **B725** (2013) 15–24, [[1305.5059](#)].
- [116] S. Fajfer and N. Košnik, *Prospects of discovering new physics in rare charm decays*, *Eur. Phys. J.* **C75** (2015) 567, [[1510.00965](#)].
- [117] LHCb collaboration, R. Aaij et al., *Search for $D_s^+ \rightarrow \pi^+ \mu^+ \mu^-$ and $D_s^+ \rightarrow \pi^- \mu^+ \mu^+$ decays*, *Phys. Lett.* **B724** (2013) 203–212, [[1304.6365](#)].
- [118] UTFIT collaboration, M. Bona et al., *Model-independent constraints on $\Delta F = 2$ operators and the scale of new physics*, *JHEP* **03** (2008) 049, [[0707.0636](#)].
- [119] R. Fleischer, *Flavour Physics and CP Violation: Expecting the LHC*, in *High-energy physics. Proceedings, 4th Latin American CERN-CLAF School, Vina del Mar, Chile, February 18-March 3, 2007*, pp. 105–157, 2008. [[0802.2882](#)].
- [120] T. Inami and C. S. Lim, *Effects of Superheavy Quarks and Leptons in Low-Energy Weak Processes $K_L \rightarrow \mu \bar{\mu}$, $K^+ \rightarrow \pi^+ \nu \bar{\nu}$ and $K^0 \leftrightarrow \bar{K}^0$* , *Prog. Theor. Phys.* **65** (1981) 297.
- [121] J. Aebischer, M. Fael, C. Greub and J. Virto, *B physics Beyond the Standard Model at One Loop: Complete Renormalization Group Evolution below the Electroweak Scale*, [[1704.06639](#)].
- [122] M. Ciuchini, E. Franco, S. Mishima and L. Silvestrini, *Electroweak Precision Observables, New Physics and the Nature of a 126 GeV Higgs Boson*, *JHEP* **08** (2013) 106, [[1306.4644](#)].
- [123] J. A. Casas and A. Ibarra, *Oscillating neutrinos and $\mu \rightarrow e \gamma$* , *Nucl. Phys.* **B618** (2001) 171–204, [[hep-ph/0103065](#)].
- [124] I. Esteban, M. C. Gonzalez-Garcia, M. Maltoni, I. Martinez-Soler and T. Schwetz, *Updated fit to three neutrino mixing: exploring the accelerator-reactor complementarity*, *JHEP* **01** (2017) 087, [[1611.01514](#)].
- [125] “NuFit 3.0 (2016).” www.nu-fit.org.
- [126] COMET collaboration, A. Kurup, *The COherent Muon to Electron Transition (COMET) experiment*, *Nucl. Phys. Proc. Suppl.* **218** (2011) 38–43.

- [127] U. Mahanta, *Neutrino masses and mixing angles from leptoquark interactions*, *Phys. Rev.* **D62** (2000) 073009, [[hep-ph/9909518](#)].
- [128] N. Arkani-Hamed, T. Han, M. Mangano and L.-T. Wang, *Physics opportunities of a 100 TeV proton-proton collider*, *Phys. Rept.* **652** (2016) 1–49, [[1511.06495](#)].
- [129] J. Ellis, *TikZ-Feynman: Feynman diagrams with TikZ*, *Comput. Phys. Commun.* **210** (2017) 103–123, [[1601.05437](#)].